Date of publication SEP-30, 2024, date of current version AUG-14, 2024.
www.computingonline.net / computing@computingonline.net

*Print ISSN 1727-6209*
*Online ISSN 2312-5381*
*DOI 10.47839/ijc.23.3.3653*

# Analytical Neural Network System for the Helicopter Turboshaft Engines Operating Modes Classification

**SERHII VLADOV[1], ZHADYRA AVKUROVA[2,3], VASYL LYTVYN[4], YURII ZHOVNIR[4]**

[1]Kremenchuk Flight College of Kharkiv National University of Internal Affairs, Kremenchuk, 39605 Ukraine
[2]Karaganda industrial university, Temirtau, 101400 Kazakhstan
[3]L.N. Gumilyov Eurasian National University, Astana, 010008 Kazakhstan
[4]Lviv Polytechnic National University, Lviv, 79013 Ukraine

Corresponding author: Serhii Vladov (e-mail: serhii.vladov@univd.edu.ua).

**ABSTRACT** A novel neural network-based analytical system has been developed for classifying helicopter turboshaft engine operating modes during flight operations. This system utilizes a neural network architecture comprising an input layer with three neurons, two fully connected hidden layers, and an output layer with two neurons. The proposed approach demonstrates an exceptional recognition accuracy of 0.997 (99.7%) across steady-state, unsteady, and transient operating modes of helicopter turboshaft engines. A new method for training this neural network has been introduced, employing forward propagation, loss calculation, backpropagation, and weight updates, enhanced by an adaptive learning rate and the cross-entropy function as the loss criterion. The method also incorporates a novel modified Smooth ReLU activation function for hidden layer neurons. This innovation led to a near-perfect accuracy in network training and reduced the loss to 0.025 (2.5%), highlighting the high quality and reliability of the neural network in classifying engine operating modes during flight. Furthermore, it has been empirically shown that the application of this neural network significantly reduces type I errors by a factor of 2.09 to 2.14 and type II errors by 2.05 to 2.21 times compared to traditional classifiers based on ART-1 and BAM networks. This advancement marks a substantial improvement in classification accuracy and error minimization for helicopter turboshaft engine operating modes.

**KEYWORDS** helicopter turboshaft engines, flight conditions, operation mode, analytical system, neural network, classifier, classifying, recognizing.

## I. INTRODUCTION

### A. RELEVANCE OF THE RESEARCH

MODERN helicopters are complex systems where efficiency and reliability depend on main components, particularly turboshaft engines (TE). These engines must operate in various modes to meet different flight conditions and operational requirements. Accurate classification of TE operating modes is crucial for enhancing performance and safety [1, 2]. Achieving high reliability requires precise, timely data on TE operation, supported by advanced monitoring and diagnostic methods to detect deviations early [3–5]. Effective models and algorithms for classifying TE operating modes are essential for improving operational characteristics and minimizing failure risks, thereby enhancing overall flight safety [6–8].

### B. STATE-OF-THE-ART

Classification of helicopter TE operating modes can be achieved in the state space using state variables as criteria [9, 10]. However, output signal vectors include additive random measurement noise, complicating the development of classification rules insensitive to this noise. Additionally, accurately determining class boundaries is challenging due to the significant dependence on engine dynamic parameters and random disturbances [11, 12]. The Bayesian method is commonly used for classification [13, 14], but it has drawbacks, such as the need to account for extensive a priori and a posteriori information on impacts, spectral density, and measurement errors, limited classification capability to steady operating modes, and reduced quality due to errors in distribution estimates and class recognition centers.

In [15] determined that improving the gas turbine engine (turbojet engine) classification operating modes quality is achieved by increasing each class analyzed signals compactness, choosing a classified parameters space nonlinear transformation certain type. This leads to a change in the distance between classes and an increase in class proximity measures in the selected metric [15]. Currently, the gas turbine engine operating modes classification is usually carried out manually, involving a highly qualified specialist. However, this work can be lengthy and monotonous, which can lead to errors and waste of time.

In [16], a gas turbine engine diagnosing method was developed and tested using a physical model based on 0-

dimensional system analysis, which effectively detects faults in engine components with high accuracy. However, the method's disadvantage in its reduced ability to classify different engine operating conditions accurately, leading to decreased diagnostic accuracy under unexpected or transient conditions.

In [17], a data-driven troubleshooting framework was developed for the fuel delivery system and gas turbine sensor measurements, using machine learning classifiers. It was compared with methods like support vector machines, linear discriminant analysis, K-neighbors, and decision trees, demonstrating its benefits through simulation. However, the framework is limited in accurately classifying conditions other than those on which it was trained, potentially reducing diagnostic accuracy when encountering new or changing conditions.

In [18], a high-reliability thrust estimation method for gas turbine engine direct thrust control was proposed, combining a physical module and an error-compensating module to account for factors like sensor noise and atmospheric changes, demonstrating high accuracy and reliability compared to existing methods. However, this method may be limited in adapting to changing engine operating conditions or new modes not represented in the training data set, affecting its operating modes classification.

Thus, various diagnostic approaches for gas turbine engines, including physical models, machine learning frameworks, and thrust estimation techniques, exhibit high precision in fault detection but may encounter challenges in accurately classifying operating states, diminishing performance in unforeseen or novel scenarios.

The development of neural network methods for classifying helicopter TE operating modes is a promising direction in aviation technology. Neural networks can process large datasets and identify hidden patterns that traditional methods may miss, especially in complex and dynamic helicopter operations, enhancing safety and system reliability [19–21]. The main task of neural network classification is to divide the observed data set into classes corresponding to different helicopter TE operating modes, analyzing parameters like temperature, pressure, and speed. Classification accuracy and speed are crucial as they influence operational decisions during flight [22, 23]. Neural networks can significantly enhance the diagnosing and monitoring process of helicopter TE operational status by automating and optimizing engine control, leading to increased efficiency and safety [24–26]. They adapt to changing conditions by analyzing large datasets from various sensors, accurately determining the current operating mode, and predicting deviations to prevent accidents [27]. Automating classification and diagnosis reduces reliance on the human factor, minimizing errors due to fatigue or inattention and speeding up data analysis, which is crucial for flight safety [28, 29].

It is worth noting that for the helicopter TE classifying operating modes task solving, a hybrid neural network based on the ART-1 and BAM networks was developed in [30], which allows adding new classes of data to long-term memory without deleting those already saved. However, this approach has critical limitations:

1. High computational costs, mean that hybrid neural networks can require significant computational resources, which can be problematic for real-time data processing on board a helicopter.

2. Setting up and training hybrid neural networks is complex and requires significant effort to ensure the stable and helicopter TE's reliable operation in various operating conditions.

3. Problems with scalability consist that as the data classes number and the information increases amount, problems may arise with the system scalability, which can reduce its efficiency and performance.

4. Hybrid neural networks effectiveness is highly dependent on the quality and the data used completeness to train them. Missing or corrupted data can significantly impact classification accuracy.

5. The results obtained from hybrid neural networks can be difficult to interpret and analyze, which can make it difficult to identify and correct errors in the system.

6. Hybrid neural networks may require prior information significant amounts for initial training, which is not always possible to provide in real operating conditions.

These limitations highlight the need for more effective neural network classification methods for helicopter TE operating modes, ensuring high accuracy and reliability under flight conditions. An analytical system based on these methods will be crucial for monitoring and diagnosing gas turbine engines, enabling timely detection and correction of deviations from the norm.

### C. MAIN ATTRIBUTES OF THE RESEARCH

The ***object*** of the research is the helicopter TE operating modes classification.

The ***subject*** of the research includes methods and analytical systems for helicopter TE operating modes classification.

The research ***aims*** to develop a method for the helicopter TE operating modes neural network classification at flight conditions, based on the advanced algorithms and analyt-ical systems integration that can effectively adapt to changing flight conditions and pro-vide high accuracy in determining the engine's current state. To achieve this aim, the following scientific and practical tasks were solved:

1. Mathematical description of TE operating modes classifying task at flight conditions.

2. The helicopter TE operating modes classifying task at flight conditions analytical system development.

3. Development of helicopter TE operating modes at flight conditions neural network classifier.

4. Development of an algorithm for training a neural network classifier of helicopter TE operating modes at flight conditions.

5. Conducting a computational experiment for the helicopter TE operating modes classifying.

6. Carrying out a comparative analysis with the most approximate analogue, implemented in the ART-1 and BAM networks form [30].

Thus, the ***main contribution*** of the research is the research is the development of a neural network analytical system for the helicopter TE operating modes classifying at flight operation, which, thanks to the neural network technologies use, allows one to the helicopter TE recognize steady-state, unsteady and transient modes with high accuracy, which, in turn, allows crew commanders make the right decisions to carry out the flight with high accuracy.

## II. MATERIALS AND METHODS

### A. MATHEMATICAL DESCRIPTION OF HELICOPTER TURBOSHAFT ENGINES OPERATING MODES CLASSIFYING TASK AT FLIGHT CONDITIONS

According to [15], the helicopter TE dynamic behaviour is described by a system of equations in the state space:

$$\dot{X}(t) = F\big(X(t), U(t), V(t), A(t)\big), \quad (1)$$

$$Y(t) = G\big(X(t), U(t), V(t)\big), \quad (2)$$

where, according to [15, 30], $X(t)$ is the engine state variables vector; $U(t)$ is the control actions vector; $V(t)$ is the disturbing external influences vector; $Y(t)$ is the observed (initial) coordinates vector; $F$ and $G$ are the nonlinear vector functions. Then the main reasons for changes in engine states can be considered as changes in the vectors $U(t)$ and $V(t)$, the helicopter TE parameters $A(t)$, as well as changes in operators $F$ and $G$ during its operation.

These equations correspond to an oriented graph displaying the changing helicopter TE modes stages (Fig. 1), where $H_1$ is the steady-state modes class for which $U(t)$ = const, $A(t)$ = const, $F(t)$ = const; $H_2$ is the regimes class accompanied by a parameters linear trend, for which $U(t)$ = const, $A(t)$ = var, $F(t)$ = var; $H_3$ is the transient operating modes class (states), for which $U(t)$ = var, $A(t)$ = const, $F(t)$ = const; $H_4$ is the unspecified operating modes class (acceleration, throttling), for which $U(t)$ = var, $A(t)$ = var, $F(t)$ = var [15, 30].

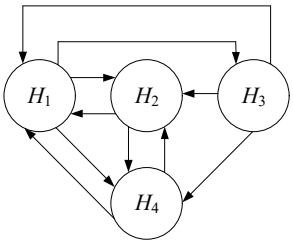


Figure 1. Helicopter turboshaft engines change classes state process model [15, 30].

The variables in (1)–(2) represent a time series formed by data sets based on the measuring results of the helicopter TE thermogas-dynamic parameters $y_1(t), y_2(t), \ldots, y_N(t)$ at a certain observation interval $t \in [t_1, t_2]$, similar to [15, 30], allows us to identify its characteristic sections corresponding to certain classes $S_1$, $S_2$, …, $S_k$ of helicopter TE states $\bigcup_{\alpha=1}^{k} S_\alpha = S_0$, where $S_0$ is the possible modes class (serviceable states).

The procedure for solving this task using a neural network is shown in Fig. 2, where $F(t)$ is the neural network desired initial reactions vector: $F(t) = \{F_1(t), F_2(t), \ldots, F_M(t)\}$, $\xi_1 \ldots \xi_M$ are the neural network outputs; $\varepsilon_1(t) \ldots \varepsilon_M(t)$ are the error vector values at the neural network output.

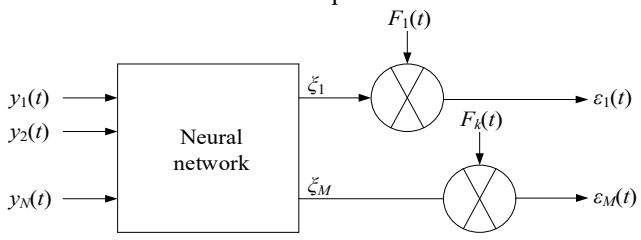


Figure 2. Helicopter turboshaft engines operating modes neural network classifier universal diagram [15, 30].

According to [15, 30], neural network training comes down to the fact that the input is time series $y_1(t), \ldots, y_N(t)$ "segments" at a certain observation interval $t \in [t_i, t_{i+1}]$, belonging to the engine $S_\alpha$, ($\alpha$ = 1, 2, …, $k$) previously known classes (modes work). According to each case, the neural network generates the desired responses in the recognized class number $\alpha$ binary representation form. For example, code (0,0) at the neural network corresponds output to the helicopter TE steady-state modes class, code (0,1) to the transient modes class, and code (1,0) to the unestablished modes class, etc. In this case, depending on the helicopter TE parameters, when receiving the code (0,0) at the output, the helicopter TE steady-state modes corresponding class, the modes one is determined: nominal, first cruising, second cruising, emergency, idle mode. The minimum error ε corresponds to a trained neural network that solves the helicopter TE recognizing (classifying) operating modes task.

In this case, based on the described modes classification ($H_1$, $H_2$, $H_3$, $H_4$) and the output codes of the neural network (for example, (0, 0) for steady-state modes, (0, 1) for transient modes, etc.), it is possible to determine, which operating modes have the greatest impact on the helicopter TE components wear.

To do this, it is necessary to assess how each operating mode affects the helicopter TE main components' wear. This can be done based on historical operational data or experimental data. For example, steady-state mode ($H_1$) corresponds to minimal wear, modes with a linear trend ($H_2$) correspond to moderate wear, transient modes ($H_3$) correspond to significant wear due to changes in parameters, and unspecified modes ($H_4$) correspond to maximum wear due to frequent changes in parameters. For the modes of each class, wear coefficients $K_{H1}$ $K_{H2}$, $K_{H3}$, and $K_{H4}$ are introduced, which will characterize the wear degree in each mode. Then the accumulated wear model is represented as the time spent on products sum in each mode and the corresponding wear coefficients:

$$W = K_{H1} \cdot T_{H1} + K_{H2} \cdot T_{H2} + K_{H3} \cdot T_{H3} + K_{H4} \cdot T_{H4}, \quad (3)$$

where $W$ is the general wear, $T_{H1}$ $T_{H2}$, $T_{H3}$, $T_{H4}$ are the time spent in modes $H_1$, $H_2$, $H_3$ and $H_4$ respectively.

To generate accurate class numbers binary representations for the steady-state prompt and reliable recognition, transient and unestablished modes, as well as determining specific modes within steady-state ones, such as nominal or cruising modes, which minimizes classification error and improves engine condition diagnostics and monitoring, it is proposed to develop the neural network training analytical system consists based on the time series "segments" corresponding to the helicopter TE operating modes various classes.

### B. THE HELICOPTER TURBOSHAFT ENGINES OPERATING MODES CLASSIFYING TASK AT FLIGHT CONDITIONS ANALYTICAL SYSTEM DEVELOPMENT

The proposed analytical system for the helicopter TE classifying operating modes (Fig. 3, 4) is an integrated approach, including the neural networks [31, 32] and advanced data analysis methods [33–35] use. The system is based on a mathematical model (1)–(2), which allows for the helicopter TE's various operating modes' accurate identification and classification without the need to modify the neural network itself. The system integrates dynamic data processing and optimization algorithms to improve classification accuracy and reliability. This provides the ability to quickly monitor and

diagnose engine conditions in real-time, which is critical to ensuring the helicopter operations' safety and efficiency.

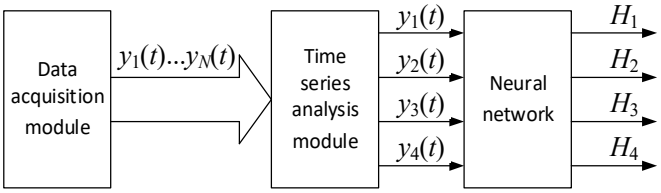


Figure 3. Proposed analytical system for the helicopter turboshaft engines classifying operating modes (proposed structural scheme) (author's research).

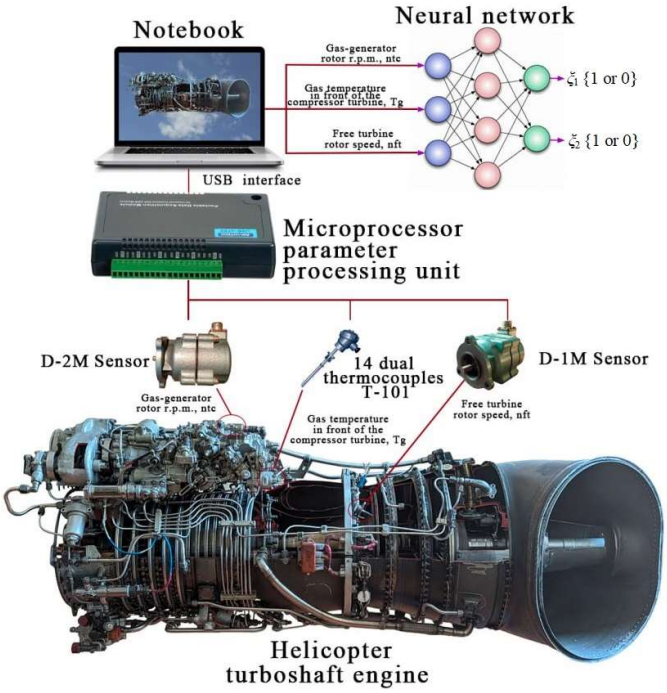


Figure 4. Proposed analytical system for the helicopter turboshaft engines classifying operating modes (proposed experimental equipment) (author's research).

The data acquisition module reads and preprocesses the parameters $y_1(t)$, $y_2(t)$, …, $y_N(t)$ time series over the observation interval $t \in [t_1, t_2]$. In this module, measured data $y_i(t)$ for each $i$-th parameter ($i$ = 1, 2, ..., $N$) are collected from sensors installed on helicopter gas turbine engines. It is noted that the gas-generator rotor r.p.m. $n_{TC}(t)$ is recorded on board the helicopter using the D-2M sensor, the free turbine rotor speed $n_{FT}(t)$ is recorded using the D-1M sensor, the gas temperature in front of the compressor turbine $T_G^*(t)$ – using a sensor consisting of 14 T-101 thermocouples [36]. Time series are represented as discrete values:

$$y_i = y_i(t_1), y_i(t_2), \dots, y_i(t_n), \tag{4}$$

where $t_1$, $t_2$, …, $t_n$ are time points in the observation interval.

For each time series, filtering is applied using the moving average method, which allows you to smooth out short-term fluctuations and highlight a more stable trend, improving the subsequent analysis and classification accuracy:

$$\hat{y}_i(t) = \frac{1}{2 \cdot k + 1} \cdot \sum_{j=-k}^{k} y_i(t + j), \tag{5}$$

where $k$ is the filter window size.

To ensure comparability, the parameter values are normalized as:

$$y_i^{norm}(t) = \frac{y_i(t) - \mu_i}{\sigma_i}, \tag{6}$$

where $\mu_i$ and $\sigma_i$ are the parameter $y_i(t)$ mean and standard deviation, respectively.

In this case, the detection and elimination of the anomalous value that may distort the analysis is performed according to the conditions:

$$If\ |y_i(t) - \mu_i| > \lambda \cdot \sigma_i, then\ y_i(t) = \mu_i, \tag{7}$$

where $\lambda$ is the threshold coefficient for determining anomalies.

It is noted that the time series decomposition into components is an important stage of analysis, which allows one to identify trends and cyclical components, improving interpretability and identifying hidden patterns in the data. In this case, it is advisable to use the expression:

$$y_i(t) = T_i(t) + S_i(t) + \epsilon_i(t), \tag{8}$$

where $T_i(t)$ is the trend, $S_i(t)$ is the seasonal component, $\epsilon_i(t)$ is the random error. The seasonal component in the helicopter TE operating modes classification context represents regular and repeated changes in thermogas-dynamic parameters that indicate cyclic engine operating modes associated with repeated operating conditions or standard operating procedures [37].

The training sample formation is carried out by dividing time series into training samples corresponding to known engine operating modes. In this case, the following expression is valid:

$$\boldsymbol{X}_i = \{y_i(t), S_i\}_{t \in [t_1, t_2]}, \tag{9}$$

where $S_i$ is the operating mode class label for time interval $t$.

The time series analysis module performs complex data processing aimed at identifying key characteristics and areas in which helicopter TE reflects various operating modes.

The helicopter TE time series parameters segmentation into sections corresponding to the operation of different classes is carried out using threshold values or algorithms that take into account dynamic changes in engine parameters.

At a steady state ($H_1$), the engine parameters remain stable within values certain range. In this case, a criterion for the parameter values stability is applied in the form:

$$if\ max\big(y_i(t)\big) - min\big(y_i(t)\big) < \epsilon_{H1}, then\ class\ H_1, \tag{10}$$

where $\epsilon_{H1}$ is the threshold for determining stability.

During transient states ($H_3$), engine parameters change dynamically, which may indicate a transition between different operating modes. One of the criteria for determining transition states is the change in the parameter rate change:

$$\text{if} \frac{dy_i(t)}{dt} > \epsilon_{H3}, \text{then class } H_3, \tag{11}$$

where $\epsilon_{H3}$ is the threshold for determining a transition state.

In unspecified modes ($H_4$), engine parameters change significantly and do not have stability or transition obvious signs. Unspecified modes are determined by the parameter's variability:

$$\text{if var}\big(y_i(t)\big) > \epsilon_{H4}, \text{then class } H_4, \tag{12}$$

where $\epsilon_{H4}$ is the threshold for determining high variability.

The helicopter TE parameters time series characteristic features identification is realized using data analysis methods [33–35]. The parameter $y_i(t)$ oscillations amplitude is defined as the difference between the maximum and minimum values over a certain time interval:

$$\text{Amplitude}\big(y_i(t)\big) = \max\big(y_i(t)\big) - \min\big(y_i(t)\big). \tag{13}$$

To estimate the parameter $y_i(t)$ oscillation frequency, spectral analysis or methods for identifying the main frequencies are used:

$$\text{Frequency}\big(y_i(t)\big) = \arg\max_f \left|\mathcal{F}\big(y_i(t)\big)\right|^2, \tag{14}$$

where $\mathcal{F}\big(y_i(t)\big)$ is the parameter $y_i(t)$ Fourier transform.

The parameter $y_i(t)$ autocorrelation function $\rho_y(k)$ at a given lag $k$ can be used to assess the current value dependence degree on previous values:

$$\rho_y(k) = \frac{E\big[\big(y_i(t) - \mu_{y_i}\big) \cdot \big(y_i(t-k) - \mu_{y_i}\big)\big]}{\sigma_{y_i}^2}, \tag{15}$$

where $\mu_{y_i}$ is the average parameter $y_i(t)$ value, $\sigma_{y_i}^2$ is the parameter $y_i(t)$ standard deviation.

Cluster analysis is used to time series group regions that exhibit similar behavioural and dynamic characteristics [38, 39]. In this case, to assess the similarity between time series $y_i(t)$ and $y_j(t)$ two sections, the Euclidean distance is used:

$$D_{ij} = \sqrt{\sum_{t=t_1}^{t_2} \big(y_i(t) - y_j(t)\big)^2}, \tag{16}$$

where $t_1$ and $t_2$ are the time interval boundaries on which the analysis is performed.

To assess the linear dependence degree between time series $y_i(t)$ and $y_j(t)$ two sections, the Pearson correlation coefficient was applied. This coefficient allows you to numerically express how closely and uniquely one time series changes with another over a given time interval $[t_1, t_2]$. The Pearson correlation coefficient is defined as:

$$\rho_{ij} = \frac{\sum_{t=t_1}^{t_2} \big(y_i(t) - \bar{y}_i\big) \cdot \big(y_j(t) - \bar{y}_j\big)}{\sqrt{\sum_{t=t_1}^{t_2} \big(y_i(t) - \bar{y}_i\big)^2} \cdot \sqrt{\sum_{t=t_1}^{t_2} \big(y_j(t) - \bar{y}_j\big)^2}}, \tag{17}$$

where $\bar{y}_i$ and $\bar{y}_j$ are the time series sections $y_i(t)$ and $y_j(t)$ average values.

To calculate each point to the centroid's proximity, consisting metric Euclidean distance and Pearson correlation coefficient combination is proposed. Let $x = (x_1, x_2, \ldots, x_n)$ be the point $x$ attributes, $c = (c_1, c_2, \ldots, c_n)$ be the centroid attributes. Then the combined metric is defined as the Euclidean distance and the Pearson correlation coefficient weighted sum according to the expression:

$$\text{Comb. metric}(x, c) = \omega \cdot D_{(x,c)} + (1 - \omega) \cdot \rho_{(x,c)}, \tag{18}$$

where $0 \le \omega \le 1$ is the weighting factor that determines the Euclidean distance compared to the Pearson correlation coefficient importance.

The proposed combined metric allows one to take into account both the spatial distance between points and centroids and their temporal correlation characteristics when performing the helicopter TE parameters time series cluster analysis.

**Consequence.** When $\omega = 1$, the combined metric (17) minimizing is equivalent to minimizing the Euclidean distance between point $x$ and centroid $c$. This means that clustering based on the combined metric with minimizing = 1 is equivalent to clustering based solely on the points by Euclidean distance spatial separation.

The time series classification module using a pre-trained neural network is a method based on transferring knowledge obtained from a pre-trained model to automatically classify sections of a time series into predefined classes $S_1$, $S_2$, ..., $S_k$. It is basis is a neural network classifier capable of efficiently processing temporary data and identifying their characteristics in the context of the classification task.

### C. DEVELOPMENT OF HELICOPTER TURBOSHAFT ENGINES OPERATING MODES AT FLIGHT CONDITIONS NEURAL NETWORK CLASSIFIER

The main thermogas-dynamic parameters recorded on board the helicopter are: the gas-generator rotor r.p.m. $n_{TC}$, the gas temperature in front of the compressor turbine $T_G^*$, the free turbine rotor speed $n_{FT}$. For three input parameters ($n_{TC}$, $T_G^*$, $n_{FT}$), based on [40, 41], the neural network classifier has the form shown in Fig. 5, where $\Delta$ is the time delay ($\Delta t = 1$ second).

According to Fig. 3, 4, the neural network must have $2 \times L$ inputs $L$ for each of the parameters: $n_{TC}$, $T_G^*$, $n_{FT}$. The specified $L$ parameters are the measured parameters $n_{TC}$, $T_G^*$, $n_{FT}$, as well as delayed values. The outputs of the neural network are signals $\xi_1$ and $\xi_2$. For a trained network, the outputs should take the values $F_1$ and $F_2$ (Table 1).

**Table 1. Neural network classifier output values (author's research, based on [15, 30])**

| Recognized modes | Neural network output signals | |
|---|---|---|
| | $F_1$ | $F_2$ |
| Steady-state class | 0 | 0 |
| Unspecified mode class | 1 | 0 |
| Transient class | 0 | 1 |

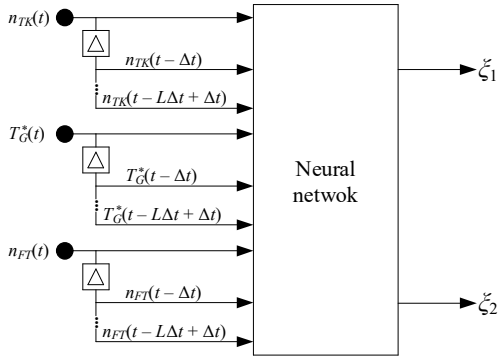


Figure 5. Proposed neural network classifier generalized architecture (author's research, based on [15, 30]).

To implement the generalized architecture of the proposed neural network classifier (Fig. 5), the work proposes the use of a neural network of such an architecture (Fig. 6):

1. An input layer consisting of three neurons corresponding to the parameters $n_{TC}$, $T_G^*$, $n_{FT}$, supplemented with corresponding delay lines.

2. In the first hidden layer, which is a fully connected layer

with 64 neurons, the activation function is Smooth ReLU of the form [36]:

$$f(x) = \begin{cases} x, & \text{if } x > 0, \\ \dfrac{1}{1 + e^{-\gamma \cdot x}}, & \text{if } x \le 0, \end{cases} \tag{19}$$

where $\gamma$ is a parameter that determines the "degree of smoothness" of the function. For $x > 0$, Smooth ReLU is a traditional ReLU [42]. For $x \le 0$, Smooth ReLU uses a sigmoid function to smoothly transition from 0 to negative values. The proposed neural activation function Smooth ReLU retains the ReLU advantages (no gradient for positive values), avoids sharp gradient "steps" and adds smoothness for negative values, which speeds up neural network training [36].

The novel activation function, Smooth ReLU, which is a derivative of the ReLU function, represents a proprietary advancement. This ReLU modification aims to create a smoother and more continuous activation function to enhance the convergence process and training stability. The proposed adjustment markedly improves neural network performance, particularly in deep learning tasks where stability and convergence speed are crucial, as validated by the experimental results presented in [36].

3. The second hidden layer, which is a fully connected layer with 32 neurons, activation function – Smooth ReLU (18).

4. The output layer is a fully connected layer with two neurons and a Softmax activation function to obtain the probability distribution of the three possible output combinations (0,0), (1,0) and (0,1).

The proposed neural network classifier architecture accounts for time dependencies in the input data sequence with delays. Three input features are processed to reveal hidden temporal patterns. Hidden layers with Smooth ReLU activation introduce nonlinearity, capturing complex dependencies. An output layer with Softmax activation and two neurons classify the data into three mutually exclusive categories: (0, 0), (1, 0), and (0, 1). This approach balances generalization and accuracy in classifying helicopter TE operating modes.

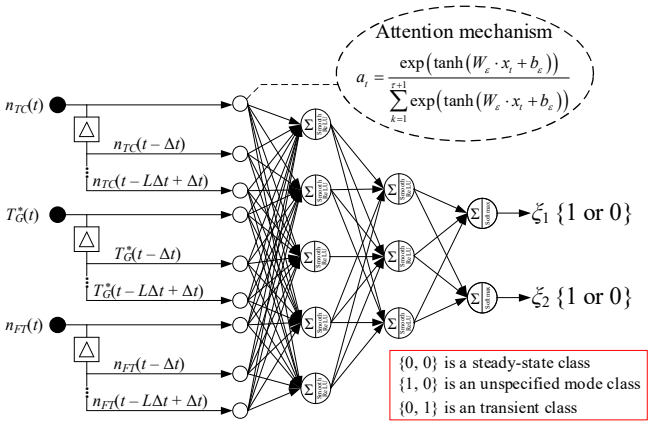


Figure 6. Helicopter turboshaft engines operating modes at flight conditions neural network classifier proposed architecture (author's research).

### *D. DEVELOPMENT OF AN ALGORITHM FOR TRAINING A NEURAL NETWORK CLASSIFIER OF HELICOPTER TURBOSHAFT ENGINES OPERATING MODES AT FLIGHT CONDITIONS*

At the data preparation stage, the training sample $\{x^{(i)}, y^{(i)}\}_{i=1}^{m}$, where $\mathbf{X} = \left(n_{TC}^{(i)}, T_G^{*(i)}, n_{FT}^{(i)}\right)$ is the helicopter TE thermogas-dynamic parameters $n_{TC}$, $T_G^*$, $n_{FT}$ values vector, $y^{(i)}$ is the target class for the $i$-th value $n_{TC}$, $T_G^*$, $n_{FT}$, is specified. Helicopters TE thermogas-dynamic parameters $n_{TC}$, $T_G^*$, $n_{FT}$ values normalization is carried out according to the expression (5).

The training sample data in the time sequences form taking into account delays is organized in the form of time sequences taking into account delays through the "time-delay embedding" method use. After applying the delay line, the input vector $\mathbf{X}$ is converted to $\mathbf{X}'$ as:

$$\begin{aligned} \mathbf{X}' = \big(&x_{norm}^{(1)}(t), x_{norm}^{(1)}(t-1), \ldots x_{norm}^{(1)}(t-\tau), \\ &x_{norm}^{(2)}(t), x_{norm}^{(2)}(t-1), \ldots x_{norm}^{(2)}(t-\tau), \\ &x_{norm}^{(3)}(t), x_{norm}^{(3)}(t-1), \ldots x_{norm}^{(3)}(t-\tau)\big), \end{aligned} \tag{20}$$

where $\mathbf{X}$ is a vector representing the time sequence of helicopters TE thermogas-dynamic parameters $n_{TC}$, $T_G^*$, $n_{FT}$ at time $t$, $\tau$ is the time delay (lag), and $m$ is the dimension or number of delays taken into account in the analysis. The delay line applying result is a vector $\mathbf{X}'$ with dimension $3 \times (\tau + 1)$.

The proposed training algorithm innovation is the proposal to introduce an attention mechanism based on time sequences. This approach allows the neural network to focus on the most significant time steps when classifying helicopter TE operating modes, improving the model's accuracy and interpretability. The attention mechanism allows the model to highlight the most important points in time in data sequences. This is especially useful for processing time series, where not all time points are equally relevant to the decision. An attention module is added between the input vector $\mathbf{X}'$ and the first hidden layer. The attention module will calculate weighting coefficients for each time point, determining its importance for the current task, that is:

$$e_t = \tanh(W_\epsilon \cdot x_t + b_\epsilon), \tag{21}$$

$$a_t = \frac{\exp(e_t)}{\sum_{k=1}^{\tau+1} \exp(e_t)}, \tag{22}$$

where $W_\epsilon$ is the weight matrix, be is the displacement vector, $e_t$ is the intermediate scoring for time point $t$, and $a_t$ is the attention weighting coefficient for point $t$.

The context vector is calculated as follows:

$$c = \sum_{t=0}^{\tau} a_t \cdot x_t. \tag{23}$$

The context vector $c$ is the input sequence time points weighted summation obtained using the attention mechanism. This vector $c$ is fed to the neural network's first hidden layer input, replacing the original vector $\mathbf{X}'$, allowing the network to focus on the most significant time steps during training.

Then the first hidden layer output with 64 neurons is given by:

$$\mathbf{h}_1 = \text{Smooth ReLU}(\mathbf{W}_1 \cdot \mathbf{c} + \mathbf{b}_1). \tag{24}$$

where $\mathbf{W}_1$ is a weight matrix of size $64 \times (3 \times (\tau + 1))$, $\mathbf{b}_1$ is a displacement vector of length 64.

The second hidden layer output with 32 neurons is given by:

$$\mathbf{h}_2 = \text{Smooth ReLU}(\mathbf{W}_2 \cdot \mathbf{h}_1 + \mathbf{b}_2). \tag{25}$$

where $\mathbf{W}_2$ is a weight matrix of size 32 × 64, and $\mathbf{b}_2$ is a displacement vector of length 32.

For an output layer with 2 neurons and Softmax activation, the following expressions are valid:

$$\mathbf{o} = \mathbf{W}_3 \cdot \mathbf{h}_2 + \mathbf{b}_3, \tag{26}$$

$$\hat{\mathbf{y}} = \text{Softmax}(\mathbf{o}), \tag{27}$$

where $\mathbf{W}_3$ is a weight matrix of size 2 × 32, $\mathbf{b}_3$ is a displacement vector of length 2, $\hat{\mathbf{y}}$ is the predicted probabilities vector for each class.

For the helicopter TE operating modes classifying task using Softmax activation, it is advisable to apply the cross-entropy function, since it effectively measures the difference between the classes' true distribution and the model-predicted probability distribution:

$$L(\mathbf{y}, \hat{\mathbf{y}}) = -\sum_{i=1}^{2} y \cdot \log(\hat{y}), \tag{28}$$

where $\mathbf{y}$ is the true class label, $\hat{\mathbf{y}}$ is the predicted class probability.

In this case, Adam's algorithm is used to minimize the loss function [43]. For each layer $l$, the weights are updated according to the following expressions:

$$\begin{aligned} \mathbf{m}_t^{\mathbf{W}_l} &= \beta_1 \cdot \mathbf{m}_{t-1}^{\mathbf{W}_l} + (1-\beta_1) \cdot \frac{\partial L}{\partial \mathbf{W}_l}, \\ \mathbf{m}_t^{\mathbf{b}_l} &= \beta_1 \cdot \mathbf{m}_{t-1}^{\mathbf{b}_l} + (1-\beta_1) \cdot \frac{\partial L}{\partial \mathbf{b}_l}, \end{aligned} \tag{29}$$

$$\begin{aligned} \mathbf{v}_t^{\mathbf{W}_l} &= \beta_2 \cdot \mathbf{v}_{t-1}^{\mathbf{W}_l} + (1-\beta_2) \cdot \left(\frac{\partial L}{\partial \mathbf{W}_l}\right)^2, \\ \mathbf{v}_t^{\mathbf{b}_l} &= \beta_2 \cdot \mathbf{v}_{t-1}^{\mathbf{b}_l} + (1-\beta_2) \cdot \left(\frac{\partial L}{\partial \mathbf{b}_l}\right)^2, \end{aligned} \tag{30}$$

$$\hat{\mathbf{m}}_t^{\mathbf{W}_l} = \frac{\mathbf{m}_t^{\mathbf{W}_l}}{1-\beta_1^l}, \hat{\mathbf{m}}_t^{\mathbf{b}_l} = \frac{\mathbf{m}_t^{\mathbf{b}_l}}{1-\beta_1^l}, \tag{31}$$

$$\hat{\mathbf{v}}_t^{\mathbf{W}_l} = \frac{\mathbf{v}_t^{\mathbf{W}_l}}{1-\beta_2^l}, \hat{\mathbf{v}}_t^{\mathbf{b}_l} = \frac{\mathbf{v}_t^{\mathbf{b}_l}}{1-\beta_2^l}, \tag{32}$$

$$\mathbf{W}_l = \mathbf{W}_l - \alpha_t \cdot \frac{\hat{\mathbf{m}}_t^{\mathbf{W}_l}}{\sqrt{\hat{\mathbf{v}}_t^{\mathbf{W}_l}} + \epsilon}, \mathbf{b}_l = \mathbf{b}_l - \alpha_t \cdot \frac{\hat{\mathbf{m}}_t^{\mathbf{b}_l}}{\sqrt{\hat{\mathbf{v}}_t^{\mathbf{b}_l}} + \epsilon}, \tag{33}$$

where $\beta_1$ and $\beta_2$ are the Adam algorithm parameters (in this work we assume $\beta_1 = 0.9$ and $\beta_2 = 0.999$ according to [44]), $\epsilon$ is a small number added for numerical stability (in this work we assume $\epsilon = 10^{-8}$), $\frac{\partial L}{\partial \mathbf{W}_l}$ and $\frac{\partial L}{\partial \mathbf{b}_l}$ are the gradients of the loss function $L$ for the weights $\mathbf{W}_l$ and biases $\mathbf{b}_l$, respectively, $\alpha_t$ is the adaptive training rate at iteration $t$, which for the Adam algorithm is defined as:

$$\alpha_t = \eta \cdot \frac{\sqrt{1-\beta_2^l}}{1-\beta_1^l}, \tag{34}$$

where $\eta$ is the initial training rate.

Thus, the neural network training algorithm as helicopter TE operating modes neural network classifier is defined as:

1. The weights and biases initialization with random values.
2. Forward propagation is the input data passing through the model, computing each layer outputs until the predicted probabilities $\hat{\mathbf{y}}$ are obtained.
3. Calculate the loss using the loss function to calculate the difference between the predicted and true values.
4. Backpropagation is calculating the loss function gradients for the weights and each layer biases.
5. Parameter update – update weights and biases using the gradient descent algorithm.
6. Repeating steps 2–5 to achieve convergence based on reducing the loss function on the validation data set.

The training algorithm for the helicopter TE operating modes neural network classifier has several key advantages: random initialization of weights and biases reduces the local minimal risk; forward propagation efficiently computes outputs for accurate probability prediction; the loss function quantifies the difference between predicted and actual values; backpropagation precisely calculates gradients to optimize layer parameters; gradient descent systematically updates weights and biases for steady convergence; and the iterative process continuously refines the model, enhancing its generalization and classification accuracy based on validation data.

## III. CASE STUDY

### A. RESULTS OF DETERMINING AND PRE-PROCESSING THE TRAINING SAMPLE

The algorithm for solving the task of helicopter TE operating modes classifying was researched using the example of data recorded on board the Mi-8MTV helicopter for the TV3-117 TE [45–48] (Fig. 7) during a six-minute flight interval of a helicopter with a twin-engine power plant. Recognition modes of engine operation are steady-state operating modes (nominal, first cruising, second cruising, emergency, idle mode) [30].

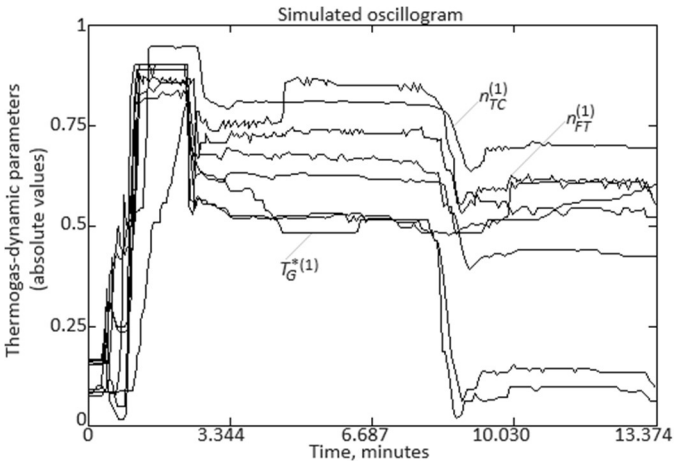


Figure 7. Diagram of the dependence of neural network classifier training error on the width of the hour window (author's research, published in [30]).

The main feature by which time series "reference" sections are identified when constructing a neural network training sample is the engine control knob position. In what follows, from the thermogas-dynamic parameters general group shown on the digitized oscillogram obtained at the Mi-8MTV helicopter flight operation mode, only those that relate to the first engine ($N = 1$) are considered: $n_{TC}^{(1)}$ is the gas-generator

rotor r.p.m. (curve 1), $n_{FT}^{(1)}$ is the free turbine rotor speed (curve 3); $T_G^{*(1)}$ is the gas temperature in front of the compressor turbine (curve 5). These data, together with the time coordinate $t$ (min), form the input vector $\mathbf{X} = \left(n_{TC}^{(1)(i)}, T_G^{*(1)(i)}, n_{FT}^{(1)(i)}\right)$, where $t \in [7.268; 13.374]$. While working with the oscillogram (Fig. 6), a training interval corresponding to two minutes was identified, within which the following modes exist: acceleration – $t_1$ = 7.268 min; $t_2$ = 7.318 min; stable (0.8 nominal) – $t_2$ = 7.318 min; $t_3$ = 8.268 min; throttling – $t_3$ = 8.268 min; $t_4$ = 8.308 min. The data was taken every second, so the training set contained 256 time samples. At the same time, the acceleration and throttling modes accounted for only five counts each. The total observation interval was 4 minutes 16 seconds (256 time counts). For high-quality classification, the width of the time window must be at least five samples to recognize operating modes classes [49]. According to the vector $\mathbf{X} = \left(n_{TC}^{(1)(i)}, T_G^{*(1)(i)}, n_{FT}^{(1)(i)}\right)$, in Table 2 presented a neural network training sample fragment.

**Table 2. Training sample fragment (author's research).**

| Number | Parameter value | | |
|---|---|---|---|
| | $n_{TC}$ | $T_G^*$ | $n_{FT}$ |
| 1 | 0.983 | 0.924 | 0.979 |
| 2 | 0.985 | 0.931 | 0.980 |
| … | … | … | … |
| 48 | 0.973 | 0.912 | 0.966 |
| … | … | … | … |
| 93 | 0.975 | 0.914 | 0.979 |
| … | … | … | … |
| 151 | 0.978 | 0.921 | 0.973 |
| … | … | … | … |
| 202 | 0.964 | 0.887 | 0.958 |
| … | … | … | … |
| 256 | 0.953 | 0.877 | 0.949 |

At the input data preparing stage (training sample preliminary analysis), the training sample homogeneity is assessed according to the Fisher-Pearson criterion [50]:

$$\chi^2 = \sqrt{\chi_1^2 + \chi_2^2}, \tag{35}$$

where $\chi_1 = \sqrt{\frac{N}{6}} \cdot Sk$, $\chi_2 = \sqrt{\frac{N}{24}} \cdot K$ are the test statistic values, where $Sk = \frac{N}{(N-1)\cdot(N-2)} \cdot \sum_{i=1} N \cdot \left(\frac{x_i - \bar{x}}{s}\right)^3$ is the sample skewness coefficient, $K = \frac{N}{(N-1)\cdot(N-2)\cdot(N-3)} \cdot \sum_{i=1} N \cdot \left(\frac{x_i - \bar{x}}{s}\right)^4 - \frac{3\cdot(N-1)^2}{(N-2)\cdot(N-3)}$ is the sample kurtosis, $s = \sqrt{\frac{1}{N-1} \cdot \sum_{i=1} N \cdot (x_i - \bar{x})^2}$ is the sample standard deviation, $\bar{x} = \frac{1}{N-1} \cdot \sum_{i=1} N \cdot x_i$ is the sample mean.

Moreover, to determine the Fisher-Pearson test critical value, the significance level $\alpha = 0.01$ was adopted in the work, which means that the type I error probability (the null hypothesis rejection when it is true) is 1 %. Thus, only 1 % of the time will we falsely reject the null hypothesis, which sets a rigour high level when testing the data homogeneity hypothesis.

In this case, the freedom degrees number for calculating the Fisher-Pearson test (also known as the Pearson goodness-of-fit test) is defined as $df = k - 1 - m$, where $k$ is the categories or intervals number in the sample, $m$ is the parameters' number to be estimated

Thus, the obtained value $\chi^2 = 3.588$ is less than the critical value is $\chi^2_{critical} = 22.362$, which confirms the samples' homogeneity and the normal distribution hypothesis.

Also, at the input data preparing stage (training sample preliminary analysis), the training sample homogeneity is confirmed according to the Fisher-Snedecor criterion [51]. To do this, a training sample of size $N = 256$ elements is randomly divided into two subsamples of size $n_1 = n_2 = \frac{N}{2} = 128$ elements each. In this case, the null hypothesis $H_0$ means the two subsamples' variances ($\sigma_1^2 = \sigma_2^2$) equality and the alternative $H_1$ means the two subsamples' variances ($\sigma_1^2 \neq \sigma_2^2$) inequality. Then the Fisher-Snedecor criterion is calculated as:

$$F = \frac{s_1^2}{s_2^2}, \tag{36}$$

where $s_1^2 = \frac{1}{N_1 - 1} \cdot \sum_{i=1}^{N_1} (x_i - \bar{x})^2$ and $s_2^2 = \frac{1}{N_2 - 1} \cdot \sum_{j=1}^{N_2} \left(x_j - \bar{x}\right)^2$ are the two-sample variance.

The obtained $F$ value is compared with the critical value $F_{critical}$ at a given significance level $\alpha = 0.01$ and freedom degrees $df_1 = N_1 - 1$, $df_2 = N_2 - 1$. If $F > F_{critical}$, then the null hypothesis is rejected, and the samples are considered heterogeneous in variance.

The resulting value is $F = 1.28$ is less than the critical value is $F_{critical} = 3.44$, which also confirms the samples' homogeneity and the normal distribution hypothesis.

The training and test samples' representativeness was evaluated through cluster analysis, which identified eight classes (Fig. 8a). Following randomization, the training and test samples were created in a 2:1 ratio (67 % and 33 %, respectively). Both samples' cluster analysis also revealed eight classes (Fig. 8b), with similar distances between clusters, confirming the samples' representativeness [38, 39].

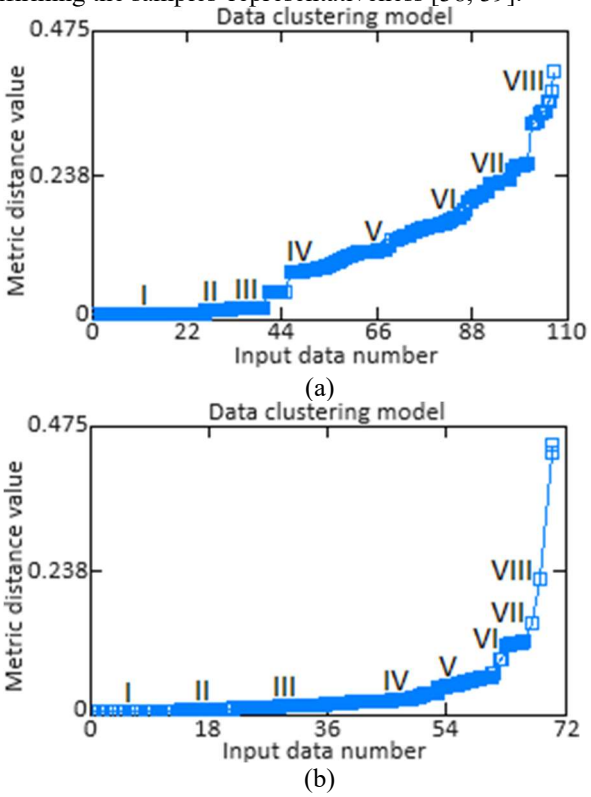


Figure 8. Cluster analysis results: (**a**) Training sample; (**b**) Test sample (author's research, published in [30]).

The helicopter TE thermogas-dynamic parameters optimal sample size determination results enabled: the training sample consists is 256 elements (100 %), the validation (control) sample comprises 172 elements (67 % of the training sample), and the test sample includes 84 elements (33 % of the training sample). In this case, for cluster analysis, a combined metric (17) was used, and the weighting coefficient was chosen to be $\omega$ = 0.05. This combined metric weight means that 95 % is metric distance and 5 % is the Pearson correlation coefficient. When varying the weighting coefficient values, for example, $\omega$ = 0.10, $\omega$ = 0.15, $\omega$ = 0.20, the classes number (8 classes) remains unchanged, however, the metric distance varies from 5.50 to 8.25 % and, at the same time, remains equal between classes. This indicates a selected weighting coefficient significant influence on the clusters' structure and emphasizes the need for parameters careful selection to achieve optimal clustering results.

When training the neural network classifier (Fig. 6), the window width was taken to be $L$ = 12, which corresponds to $3 \times L$ = 36 neural network inputs. Fig. 9 analysis shows that when the helicopter TE operating modes classification (recognition) task solving, it is enough to take the time window width equal to 8...12.

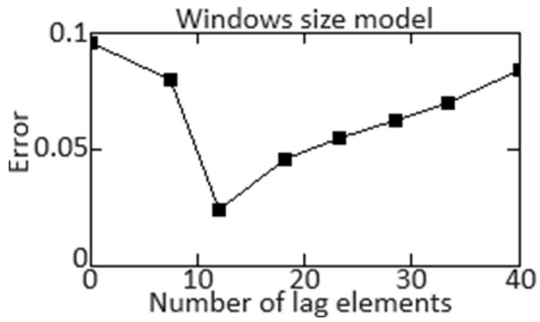


Figure 9. Diagram of the neural network classifier training error dependence on the hour window width (author's research).

### B. NEURAL NETWORK CLASSIFIER TRAINING RESULTS

The data used to train the neural network consist of the helicopter's TE thermogas-dynamic characteristics, which are captured during the helicopter's flight: gas-generator rotor r.p.m. $n_{TC}$, free turbine rotor speed $n_{FT}$, gas temperature in front of the compressor turbine $T_G^*$ (Table 2).

During the training of the neural network classifier with the proposed algorithm, the neural network accuracy (Fig. 10) loss (Fig. 11) dependences on the iterations number (200 iterations in total) were obtained. In the diagrams, the "blue curve" represents training on the training set, and the "orange curve" represents validation on the control set.

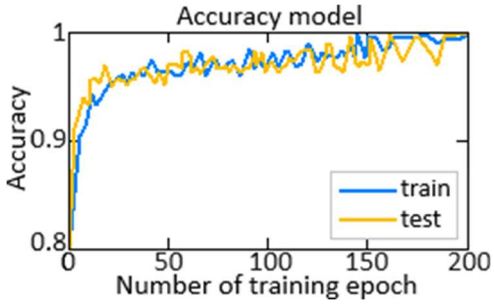


Figure 10. Diagram of the accuracy function dynamics at the model training and validation stages (author's research).

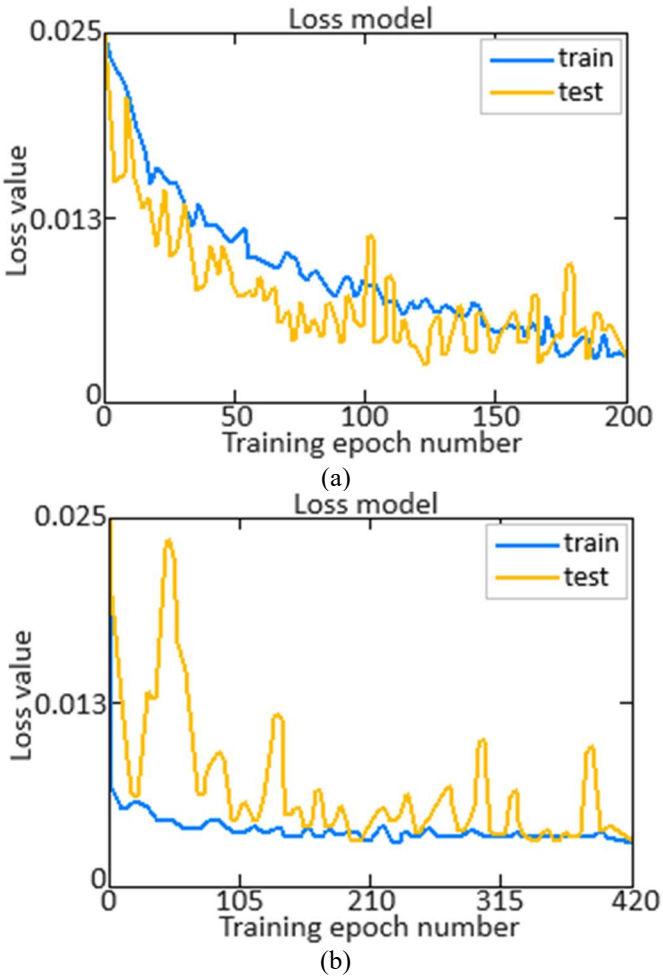


Figure 11. Diagram of the loss function dynamics at the model training and validation stages (author's research).

Fig. 10 shows that the accuracy reaches 1, and Fig. 11 that the loss does not exceed 0.025. As can be seen from Fig. 10a, the neural network training error by the developed algorithm using the Smooth ReLU activation function developed in [36] reaches its minimum is 0.0003 at 200 training epochs, while after 200 training epochs, the error remains stable and does not change its value. A similar experiment was also carried out using the developed algorithm using the traditional ReLU activation function (Fig. 10b). As can be seen from Fig. 10b, to achieve a minimum training error of 0.0003, the neural network needed 420 training epochs, which is 2.10 times more than when using the Smooth ReLU activation function developed in [36]. As can be seen from Fig. 11, the neural network training convergence was achieved with 200 training epochs using the Smooth ReLU activation function developed in [36], and with 420 training epochs using the traditional ReLU activation function. This indicates the training's high efficiency and the model's ability to generalize data with high accuracy, which makes it suitable for helicopter TE operating modes classifying.

After the neural network classifier training (Fig. 6) on a test sample (33 % of the training sample), its effectiveness was tested on a control sample (67 % of the entire sample) in the helicopter TE operating modes classifying task at flight conditions. To recognize the helicopter TE operating modes, the neural network classifier selects samples from the observations' time series values corresponding to the steady-state modes within the time window $\Delta\tilde{y}_i(t)$, by subtracting the

average value (moving average) over the entire interval $t \in [t_1; t_2]$. In steady state, $\Delta\tilde{y}_i(t)$ is equal to zero, and in other modes, it is different from zero, that is [15, 30]:

$$\Delta\tilde{y}_i(t) = \tilde{y}_i - \frac{1}{L} \cdot \sum_{i=0}^{L-1} \tilde{y}_i, \tag{37}$$

where $L$ is the "window" width, while the time window optimal size in the experimental research process.

Fig. 12 shows that the neural network classifier outputs reference values take the values 0 or 1, while the actual output signals (due to the time window moving process inertia) can take continuous values in the range [0; 1]. Therefore, according to [15, 30], the calculated values of $\xi_1$ and $\xi_2$ are rounded to the nearest integer using the following expression:

$$\bar{\xi}_i = \begin{cases} 0, \text{if } \xi_i \le 0.5, \\ 0, \text{if } \xi_i > 0.5. \end{cases} \tag{38}$$

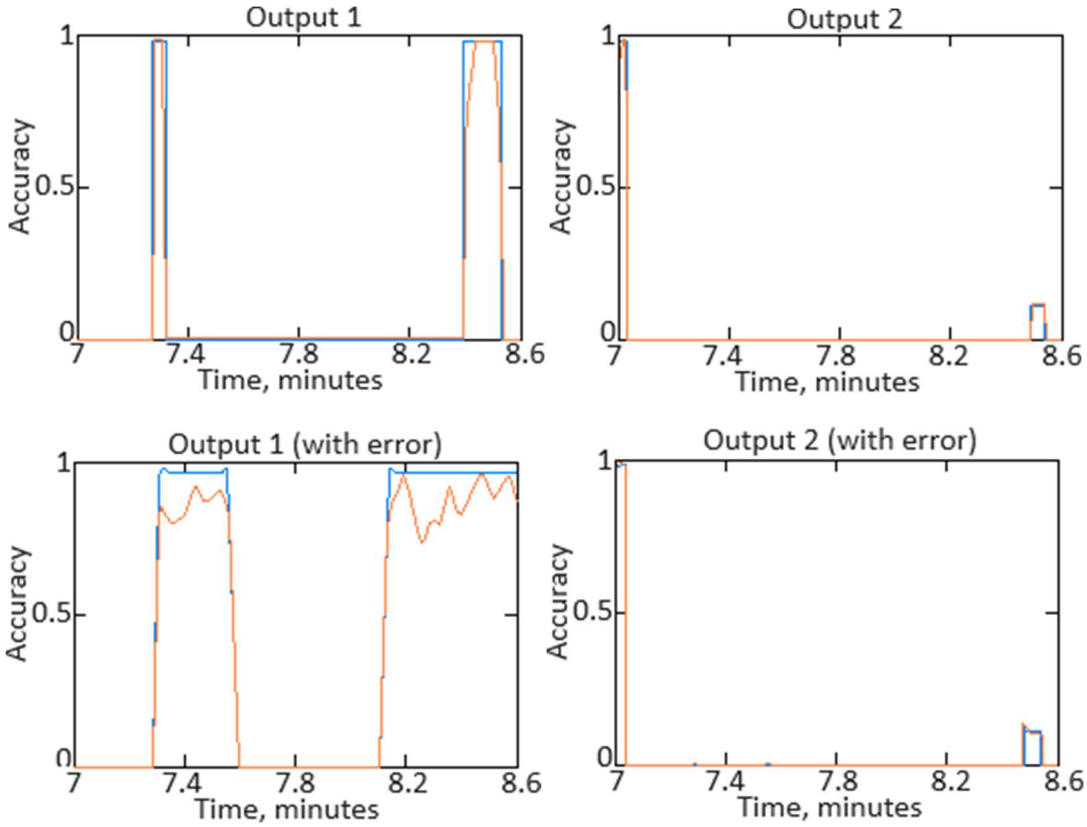


Figure 12. The TV3-117 TE operating ratings' classification diagram ("blue curve" is the etalon; "orange curve" is the proposed neural network classifier): (**a**) 1st exit ($n_{TC}$); (**b**) 2nd exit ($T_G^*$); (**c**) 1st exit ($n_{TC}$) taking into account errors; (**d**) 2nd exit ($T_G^*$) taking into account errors (author's research).

Fig. 13 shows diagrams of the helicopter TE operating modes classification quality coefficient dependence on the training epochs number, obtained from the validation sample. In this case, the quality coefficient was determined as:

$$C_{quality} = \left(1 - \frac{T_{error}}{T_0}\right) \cdot 100\%, \tag{39}$$

where $T_{error}$ is the section total time corresponding to erroneous classification; $T_0$ is the test sample duration (in our case $T_0$ = 1.6 seconds, see Fig. 12).

As can be seen from Fig. 13, the quality coefficient for recognizing the helicopter TE operating modes lies in the range from 99.95 to 99.99 % with optimal 200 neural network training epochs. This indicates the model's high accuracy, which achieves near-perfect classification levels, demonstrating stable and efficient training under the given parameters.

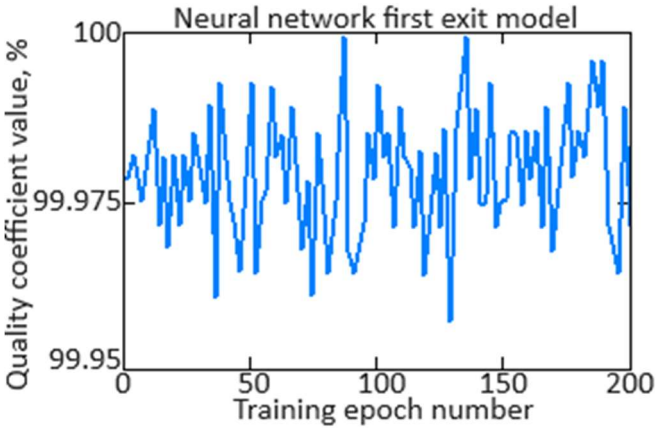


(a)

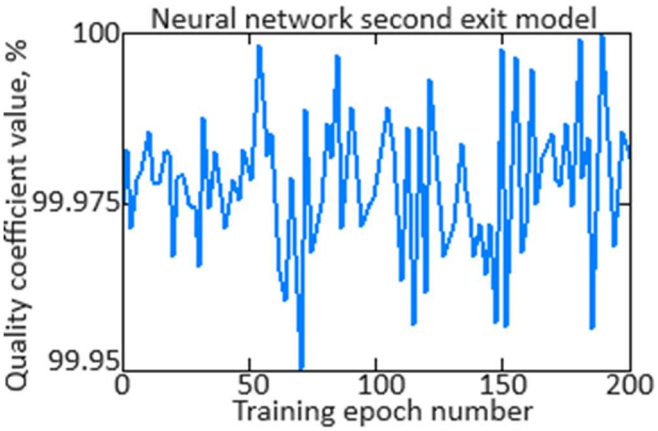


(b)

Figure 13. Diagrams of the TV3-117 TE operating modes classification quality coefficient: (**a**) 1st exit ($\xi_1$); (**b**) 2nd exit ($\xi_2$) (author's research).

Also, as a control experiment part conducted on a validation sample, regression models presented in Fig. 1 were obtained (Fig. 14).

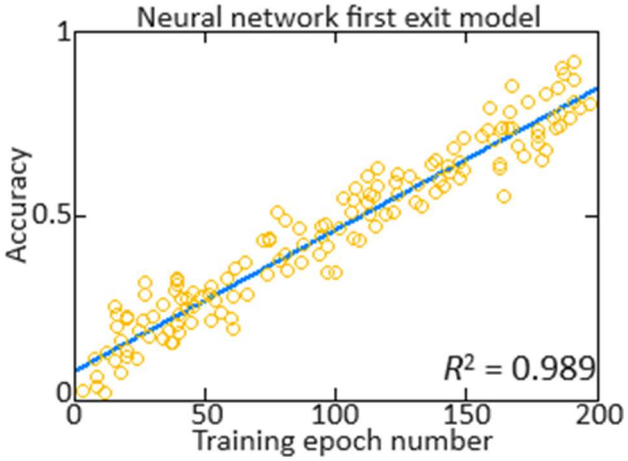


(a)

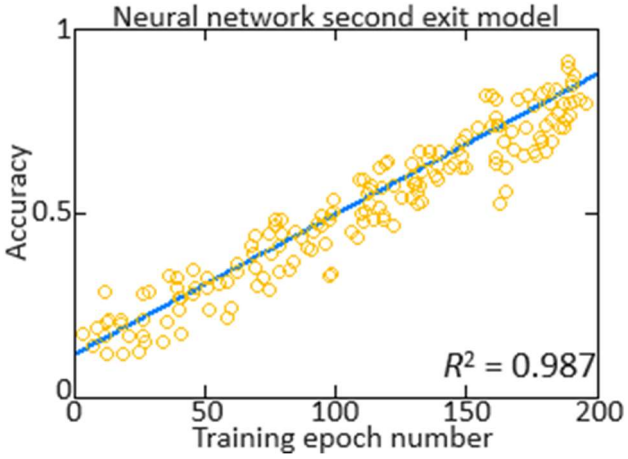


(b)

Figure 14. Diagrams of the TV3-117 TE operating modes classification quality coefficient: (**a**) 1st exit ($\xi_1$); (**b**) 2nd exit ($\xi_2$) (author's research).

In this case, the determination coefficient was $R^2 = 0.989$ (for the first output) and $R^2 = 0.987$ (for the second output). The results indicate that the model's data variation explains 98.9 % and 98.7 %, respectively. This means that the models well describe the output parameters' dependence on input data and can be effectively used in the helicopter TE operating modes classification.

The TV3-117 TE steady-state, unsteady and transient modes classification make it possible to reduce specific fuel consumption. To estimate the TV3-117 TE specific fuel consumption, a model was built in the Python programming language for 5 operating modes: nominal, first cruise mode, second cruise mode, emergency mode and idle mode.

The 'specific_fuel_consumption' function calculates the new fuel consumption based on the classification at flight operation mode and improvement factor in fuel efficiency. To train the model, a multilayer perceptron with two hidden layers was used. The data is split into training and testing sets, standardized, and then used to train a neural network model.

As a result, the TV3-117 TE specific fuel consumption comparison was obtained for the original passport data and for the data obtained when using proposed neural network classifier (Fig. 7) in the helicopter TE operating modes classification task at flight operation mode.

It is assumed that the neural network classifies operating modes based on time series $y_i(t)$, which represent data on engine parameters at a certain time $t$. In this case, the neural network generates a recognized class number binary representation: (0,0) is the steady state (for example, nominal, first cruising, second cruising, emergency, idle mode); (0,1) is the transition mode; (1,0) is the unsteady mode.

Specific fuel consumption $C_e$ is determined as the helicopter TE operating modes classification and other parameter's function:

$$C_e = f_\alpha(helicopter\ TE\ other\ parameters), \qquad (40)$$

where $f_\alpha$ is a function depending on the helicopter TE parameters specific to the operating mode $\alpha$. The results are shown in Fig. 15.

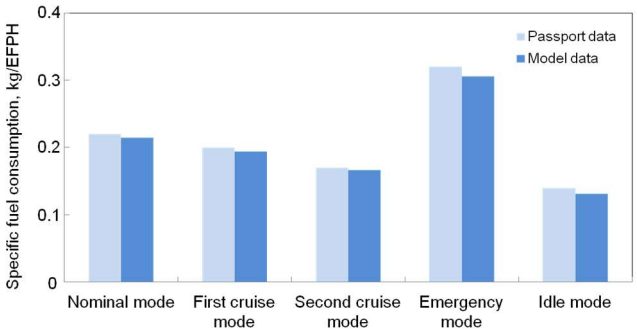


Figure 15. The TV3-117 turboshaft engine specific fuel consumption (author's research).

For each operating mode, you can use physical models [52–55] or empirical dependencies [52–55] that take into account the helicopter TE parameters influence on fuel consumption. For example:

1. In nominal mode, a model based on stable engine operation can be used.
2. Cruise modes can take into account the fuel consumption optimization at various flight speeds and altitudes.
3. In emergency idle modes, increased fuel consumption due

to changed gas turbine engine operating parameters can be taken into account.

The TV3-117 TE specific fuel consumption (Fig. 15) for the original passport data and for the data obtained when using neural network in the helicopter TE operating modes classification task at flight operation mode is less by 0.0055…0.0144 kg/EFPH.

### C. NEURAL NETWORK CLASSIFIER VALIDATION RESULTS

The obtained results validation was carried out using k-fold cross-validation, in which the obtained data (Fig. 11) is divided into $k = 8$ equal parts (folds). In $k = 8$ for each iteration, one part is used for testing, and the remaining $k - 1$ parts are used for training the model. The process is repeated $k = 8$ times and the results are averaged to obtain the final score. Partitioning the data into $k = 8$ folds is done as follows:

$$D = \{D_1, D_2, \ldots, D_k\}, \tag{41}$$

where $D$ is the original dataset and $D_i$ is the $i$-th fold.

For each $i$-th fold from 1 to $k$, the following is true:

$$Train_i = \frac{D}{D_i}, \quad Test_i = D_i. \tag{42}$$

To assess the model quality on each fold, it is assumed that $Accuracy_i$ is the quality metric on the $i$-th fold. Then the average quality metric for all folds will be equal to:

$$Average\ Metric = \frac{1}{k} \cdot \sum_{i=1}^{k} Accuracy_i. \tag{43}$$

The obtained data (Fig. 11) validation results are shown in Table 3.

**Table 3. The obtained data validation results (author's research).**

| Fold number | Metric | Font size and style | Font size and style | Font size and style | Font size and style |
|---|---|---|---|---|---|
| | | 1st exit ($n_{TC}$) (Fig. 11a) | 2nd exit ($T_G^*$) (Fig. 11b) | 1st exit ($n_{TC}$) taking into account errors (Fig. 11c) | 2nd exit ($T_G^*$) taking into account errors (Fig. 11d) |
| 1 | $Accuracy_1$ | 0.982 | 0.985 | 0.992 | 0.983 |
| 2 | $Accuracy_2$ | 0.962 | 0.972 | 0.983 | 0.985 |
| 3 | $Accuracy_3$ | 0.973 | 0.980 | 0.987 | 0.994 |
| 4 | $Accuracy_4$ | 0.984 | 0.985 | 0.991 | 0.990 |
| 5 | $Accuracy_5$ | 0.991 | 0.993 | 0.972 | 0.977 |
| 6 | $Accuracy_6$ | 0.990 | 0.991 | 0.974 | 0.978 |
| 7 | $Accuracy_7$ | 0.982 | 0.983 | 0.988 | 0.989 |
| 8 | $Accuracy_8$ | 0.984 | 0.986 | 0.980 | 0.985 |
| **Average Metric** | | **0.981** | **0.984** | **0.983** | **0.985** |

As can be seen from Table 3, the Average Metric values for the obtained results were respectively: 0.981, 0.984, 0.983, 0.985. This indicates the proposed model's accuracy high level in all four diagrams. These results demonstrate the model's reliability and stability in classifying the helicopter TE operating modes, showing minimal deviations between different folds and experiments.

High Average Metric values indicate that the model has strong generalization ability, successfully recognizing engine operating modes on both training and test samples. Thus, the proposed k-fold cross-validation methodology confirms the model's efficiency and stability, making it suitable for use in helicopter TE real operating conditions.

These results also highlight thorough validation process importance when developing machine learning algorithms for technical applications, ensuring the classification systems' accuracy and reliability.

### D. THE RESULTS OBTAINED STABILITY ASSESSING

To assess the neural network training stability, several indicators have been proposed. Some of the main ones are the gradient values, changes in the loss function and accuracy metrics on the training and validation samples [56–59].

To assess the gradients' stability, you can use their norms, for example, the $L2$ gradient norm, which is defined as:

$$\|\nabla L\|_2 = \sqrt{\sum_{i=1}^{n} \left(\frac{\partial L}{\partial \theta_i}\right)^2}, \tag{44}$$

where $\nabla L$ is the loss function $L$ gradient, and $\theta_i$ are the model parameters (weights and biases).

Stable training assumes that the loss function $L$ decreases during the training process. This can be estimated as the difference in the loss function values at two successive iterations:

$$\Delta L = L_{t-1} - L_t, \tag{45}$$

where $L_t$ is the loss function value at iteration $t$.

For a more detailed analysis, it is proposed to use the change coefficient in the loss function, which is defined as:

$$\text{Loss change ratio} = \frac{|L_{t-1} - L_t|}{L_{t-1}}. \tag{46}$$

To assess stability, it is also proposed to track changes in model accuracy on the training and validation sets:

$$\Delta\text{Accuracy} = \text{Accuracy}_t - \text{Accuracy}_{t-1}, \tag{47}$$

where $\text{Accuracy}_t$ is the model accuracy at iteration $t$.

To assess the training stability, it is also proposed to monitor metrics such as Accuracy or mean square error (*MSE*) on the validation set:

$$\Delta\text{Validation Metric} = \text{Metric}_t - \text{Metric}_{t-1}. \tag{48}$$

Stable training also implies the absence of significant fluctuations in metrics, i.e.:

$$\sigma(\Delta L) \approx 0, \sigma(\Delta\text{Accuracy}) \approx 0, \tag{49}$$

where $\sigma$ is the changes in standard deviation in loss functions or metrics.

According to the neural network training obtained results (Fig. 9, Fig. 10a), the initial data can be presented in Table 4.

**Table 4. The initial data for the neural network stability assessing (author's research)**

| Epoch | Training accuracy | Validation Accuracy | Loss |
|---|---|---|---|
| 1 | 0.950 | 0.940 | 0.025 |
| 50 | 0.970 | 0.960 | 0.010 |
| 100 | 0.985 | 0.980 | 0.005 |
| 150 | 0.990 | 0.990 | 0.002 |
| 200 | 0.995 | 0.995 | 0.0003 |

Then, according to (38)–(43), we obtain: $\Delta L_{100-101} = 0.005 - 0.0048 = 0.0002$, $\Delta L_{150-151} = 0.002 - 0.0018 = 0.0002$, Loss change ratio$_{100-101} = \frac{0.0002}{0.005} = 0.04$, Loss change ratio$_{150-151} = \frac{0.0002}{0.02} = 0.1$, $\Delta$Training Accuracy$_{100-101} = 0.985 - 0.984 = 0.001$, $\Delta$Training Accuracy$_{150-151} = 0.990 - 0.989 = 0.001$, $\Delta$Validation Accuracy$_{100-101} = 0.980 - 0.979 = 0.001$, $\Delta$Validation Accuracy$_{150-151} = 0.990 - 0.989 = 0.001$. According to the data obtained, it can be stated that losses decrease smoothly and gradually, without sudden jumps, which indicates a stable convergence of the model. At the same time, the accuracy of the training and validation samples grows steadily and reaches high values (0.995). Small changes in accuracy and loss function at each step indicate that training is proceeding without sudden changes, which also confirms stability. Thus, the neural network is trained steadily, with a smooth improvement in all key metrics.

### *E. RESULTS OF THE FIRST AND SECOND TYPES OF ERRORS' CALCULATION AND ROC ANALYSIS*

According to [15, 30], the first and second error types [60, 61] may occur, i.e., the state $S_i$ to the class $S_j$ assignment. Therefore, the work assessed the first and second types of errors in recognizing the helicopter TE operating modes. The first and second types of errors in the helicopter TE operating modes recognizing tasks are determined as follows. The first error type occurs when the neural network incorrectly classifies a steady-state mode (code 0,0) when in fact it is a transient mode (code 0,1), transient (code 1,0), or other incorrect mode. This results in erratic or abnormal engine operation being mistaken for normal, which can have serious consequences for safety and operation. The second type of error occurs when the neural network does not recognize the steady-state mode (code 0,0) and incorrectly classifies it as a transient, transient, or other incorrect mode (for example, codes 0,1 or 1,0). In this case, normal engine operation is incorrectly perceived as abnormal, which can lead to unnecessary adjustments or engine stalling. These errors can significantly affect the efficiency and safety of helicopter operations. The first and second types of errors are calculated as:

$$\alpha = \frac{FP}{FP + TN}, \beta = \frac{FN}{FN + TP}, \tag{50}$$

where *TP* (True Positive) is the steady-state mode (code 0,0) correct classifications number; *TN* (True Negative) is the unidentified modes (codes 0,1, 1,0 and others) correct classifications number; *FP* (False Positive) is the steady-state mode (code 0,0) incorrect classifications number the uninstalled one instead; *FN* (False Negative) is the unspecified mode incorrect classifications number the steady-state mode (code 0,0) instead.

The first type error null hypothesis: "The neural network correctly classifies the helicopter TE operating modes as steady-state mode (code 0,0) when they are unsteady (code 0,1, 1,0, or others)".

The second type error null hypothesis: "The neural network correctly classifies the helicopter TE operating modes steady-state mode as unestablished or transient (codes 0,1, 1,0 or others) when they are steady (code 0,0)".

Table 5 shows the helicopter TE operating modes the first and second types recognizing task error calculations comparative analysis results using the proposed neural network classifier (Fig. 5) and the neural network classifier previously developed in [30] based on the ART-1 and BAM networks.

**Table 5. The first and second errors' types calculations comparative analysis results (author's research).**

| Neural network classifier | The helicopter TE operating modes recognizing error probability, % | | | | | |
|---|---|---|---|---|---|---|
| | Steady-state mode (code 0,0) | | Transient mode (code 0,1) | | Unestablished mode (code 1,0) | |
| | The first error type | The second error type | The first error type | The second error type | The first error type | The second error type |
| Proposed neural network classifier | 0.65 | 0.34 | 0.66 | 0.36 | 0.68 | 0.39 |
| Neural network classifier based on the ART-1 and BAM networks [30] | 1.38 | 0.75 | 1.41 | 0.77 | 1.42 | 0.80 |

As can be seen from Table 5, the first error type in recognizing the helicopter TE operating modes takes values in the range from 0.66 to 0.68 % when using the proposed neural network classifier (Fig. 5). At that time, the first type error takes values in the range from 1.38 to 1.42 % when using a neural network classifier based on the ART-1 and BAM networks [30]. Thus, the developed neural network classifier use (Fig. 5) reduces the first type error by 2.09…2.14 times compared with the neural network classifier based on the ART-1 and BAM networks [30] use. Similarly, the second type error in recognizing the helicopter TE takes values in the range from 0.34 to 0.39 % when using the proposed neural network classifier (Fig. 5), and when using a neural network classifier based on the ART-1 and BAM networks [30] – in the range from 0.75 to 0.80 %. Thus, the developed neural network classifier (Fig. 5) use reduces the second type error by 2.05…2.21 times compared with the neural network classifier based on the ART-1 and BAM networks [30] use.

Based on the calculated first and second errors' types, the helicopter TE operating modes recognition accuracy is determined as:

$$Accuracy = \frac{TP + TN}{TP + TN + FP + FN}, \tag{51}$$

and the decision-making accuracy to carry out a flight is as follows:

$$Decision\ Accuracy = \frac{Correct\ Decisions}{Total\ Decisions}, \tag{52}$$

where "*Correct decisions*" is the situations set when the

decision made corresponds to the actual need for the flight (for example, the helicopter TE operating mode is correctly determined), and "*Total decisions*" is the sum of the correct and incorrect decisions.

Table 6 shows the helicopter TE operating mode recognizing accuracy calculations comparative analysis results and the flight implementation decision-making accuracy when using both the developed neural network classifier (Fig. 5) and the neural network classifier based on the ART-1 and BAM networks [30].

**Table 6. Accuracy calculations comparative analysis results (author's research).**

| Neural network classifier | Accuracy | Decision accuracy |
|---|---|---|
| Proposed neural network classifier | 0.997 | 0.973 |
| Neural network classifier based on the ART-1 and BAM networks [30] | 0.985 | 0.935 |

As shown in Table 6, the accuracy of recognizing helicopter TE operating modes using the developed neural network classifier (Fig. 5) is 0.997, which is 1.06 times higher than that achieved with a neural network classifier based on ART-1 and BAM networks [30]. Similarly, the flight decision-making accuracy with the developed classifier is 0.985, 1.05 times higher than with the ART-1 and BAM-based classifier [30]. Therefore, the developed neural network classifier (Fig. 5), used as a closed onboard helicopter TE automatic control system component [62], should effectively recognize helicopter TE operating modes under flight conditions.

To assess the classification model quality, the work used ROC analysis with the ROC curve construction. The ROC curve is constructed based on the True Positive Rate (*TPR*) and False Positive Rate (*FPR*) values at different classifier thresholds [63–65].

True Positive Rate (*TPR*) is defined as:

$$TPR = \frac{TP}{TP + FN}. \tag{53}$$

False Positive Rate (*FPR*) is defined as:

$$FPR = \frac{FP}{FP + TN}. \tag{54}$$

The area under the AUC curve is calculated using numerical methods such as the trapezoidal method. The analytical expression for numerical integration by the trapezoidal method has the form:

$$AUC = \sum_{i=1}^{n-1} (FPR_{i+1} - FPR_i) \cdot \frac{TPR_{i+1} + TPR_i}{2}, \tag{55}$$

where $n$ is the threshold's number. Table 7 and Fig. 16 shows the ROC analysis results.

**Table 7. ROC analysis results (author's research).**

| Actual \ Predicted | Proposed neural network classifier | Neural network classifier based on the ART-1 and BAM networks [30] |
|---|---|---|
| True Positives | 98 | 2 |
| True Negatives | 2 | 8 |
| False Positives | 285 | 290 |
| False Negatives | 35 | 98 |
| TPR | 0.786 | 0.029 |
| FPR | 0.018 | 0.032 |
| AUC | 0.895 | 0.567 |

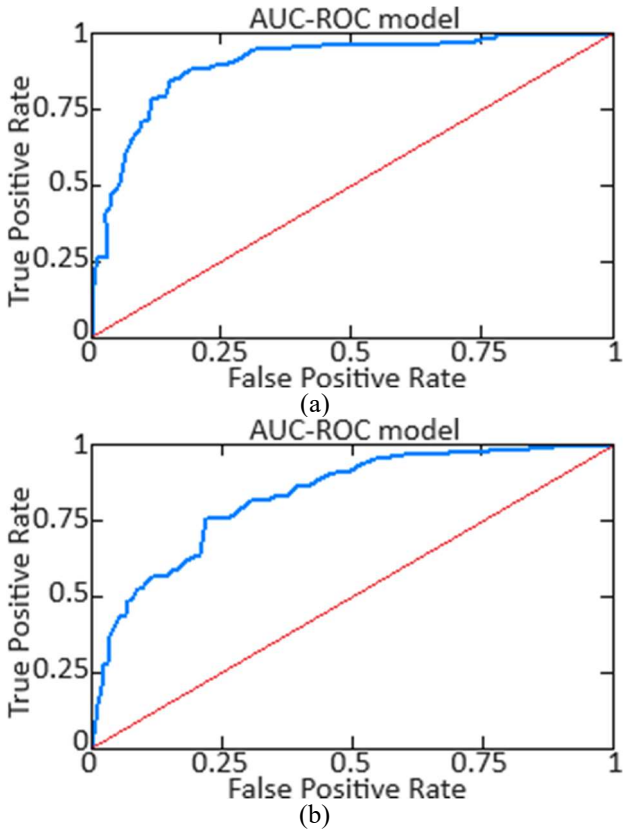


Figure 16. The AUC-ROC curve: (**a**) Proposed neural network classifier; (**b**) Neural network classifier based on the ART-1 and BAM networks [30] (author's research).

Thus, the proposed neural network classifier use gives high accuracy with false positive results at a low level; the neural network classifier based on the ART-1 and BAM networks [30] use gives moderate accuracy, with noticeable errors, and 1.58 times lower than that proposed neural network classifier.

## IV. DISCUSSION

This article represents a significant expansion and continuation of further research [30] in the development the helicopter TE operation modes classifying at flight operating conditions neural network methods and systems. Unlike [30], this article develops the helicopter TE operating modes classifying analytical system (Fig. 3, 4), which basis is a neural network classifier (Fig. 5).

Unlike [30], this article proposes the feed-forward neural network with delay lines at its input with an innovative Smooth ReLU activation function use [36]. This architecture neural network use made it possible to reduce the first type error (cases when the system mistakenly identifies an engine operation normal error mode as a transient or unsteady mode) by 2.09...2.14 times and the second type error (cases when the system does not recognize and does not signal the transients that actually occurred or unsteady engine operating modes) 2.05...2.21 times compared with a neural network classifier based on the ART-1 and BAM networks use [30] (Table 3). Even a slight reduction in the first and second types errors is critical for the helicopter TE operating modes classifying at real-time flight conditions, since this directly affects flight safety. Reducing the first type errors number prevents unnecessary interference in engine operation, which reduces the risk failures and extends the units life. Reducing the second type errors number ensures timely detection and potentially

dangerous operating modes elimination, which increases the helicopter control reliability and efficiency, minimizing the emergency situations likelihood.

Based on the traditional backpropagation algorithm, the proposed neural network training algorithm has been developed, which distinguishing feature from the traditional one is the attention mechanism introduction based on time sequences in the input layer. This made it possible to converge the neural network training with 200 training epochs, and also to the loss function value reduce from 2.5 to 0.3 % (Fig. 10). At that time, the neural network classifier based on the ART-1 and BAM networks [30] use made it possible to achieve the neural network convergence and the loss function value reduce from 2.5 to 0.3 % only with 1000 training epochs. The results obtained made it possible to increase the helicopter TE operating modes classification accuracy at flight operating conditions from 98.5 to 99.7 %, as well as to increase the decision-making on flight operations accuracy from 93.5 to 97.3 % (Table 4). This means improvements in the neural network training speed and efficiency, leading to more reliable and responsive real-time helicopter classification and control.

In addition, the helicopter TE operating modes classifying developed neural network analytical system use at flight operating conditions made it possible to determine the specific fuel consumption value according to the operating mode.

The helicopter TE operating modes classifying developed neural network analytical system use at flight operating conditions potential disadvantages are high computational costs. Training and using a neural network with the attention mechanism implementation requires significant computing resources, which can be problematic in limited hardware power conditions on board a helicopter. This may result in the need for additional hardware modifications, increased power consumption, and increased system complexity.

At the same time, in [66] the helicopter TE complex monitoring and operation control implementing on-board neural network methods possibility based on placing an electronic neural network system on board the helicopter, implemented on the Intel Core Stick 2 neural processor (Fig. 17) basis, has been proven.

Figure 17. The modified Mi-8T helicopter cabin proposed appearance (the helicopter turboshaft engines integrated monitoring and operation control proposed on-board electronic neural network system is highlighted in red) (author's research).

This allows you to significantly reduce computational costs and increase the efficiency of the system in real time. The such a processor use provides the necessary performance (the all operation execution time s, taking into account the retrieving data from memory time, is 196.246 ns, while this parameter for the Raspberry Pi NanoPi M1 Plus processor is 1589.544 ns [66]) for processing data large amounts and executing complex calculations, which makes it possible to the helicopter TE quickly monitoring [67] and operation control directly [68–73] at flight conditions.

Thus, the Intel Core Stick 2 neural processor use eliminates the helicopter TE operating modes classifying neural network analytical system above-mentioned disadvantages at the on-board implementation conditions.

## V. CONCLUSIONS

The neural network analytical system for helicopter turboshaft engines operating modes classification at flight operation mode was further researched, which differs from existing ones in that the developed neural network uses the input layer with three neurons, two fully connected hidden layers and an output layer with two neurons consisting made it possible to the helicopter turboshaft engines recognizing steady-state modes, unsteady modes and transient modes task solve with accuracy is up to

0.997 (99.7 %). This, in turn, allows the helicopter crew commander to make the right decision regarding the flight execution with an accuracy of 0.945 (94.5 %).

A neural network training method has been developed an input layer with three neurons, two fully connected hidden layers, and an output layer with two neurons consisting, based on forward propagation, loss calculation, backpropagation and updating the neural network weights, which due to the adaptive training rate, cross-entropy function as a loss function use, as well as the proposed modified function for the hidden layers Smooth ReLU activating neurons, made it possible to achieve almost the neural network training 100 % accuracy and reduce losses to 0.025 (2.5 %), which is a high indicator of the quality of work neural network in the helicopter turboshaft engines operating modes classification at flight operation mode task.

It has been experimentally proven that the proposed neural network uses, the input layer with three neurons, two fully connected hidden layers and an output layer with two neurons consisting, in the helicopter turboshaft engines operating modes classifying at flight operation mode task, reduces the first type errors by 2.09...2.14 times and the second type errors – by 2.05...2.21 times compared with the neural network classifier based on the ART-1 and BAM networks [30]. This shows the feasibility of the developed neural network used in an onboard implementation to classify the helicopter turboshaft engines' operating modes during flight operation.

## VI. ACKNOWLEDGMENTS

The research was carried out with the grant support of the National Research Fund of Ukraine "Methods and means of active and passive recognition of mines based on deep neural networks", project registration number 273/0024 from 1/08/2024 (2023.04/0024). This research also was supported by the Ministry of Internal Affairs of Ukraine "Theoretical and applied aspects of the development of the aviation sphere" under Project No. 0123U104884. Also, we would like to thank the reviewers for their precise and concise recommendations that improved the presentation of the results obtained.

## References

[1] C. Zhang, V. Gümmer, "Multi-objective optimization and system evaluation of recuperated helicopter turboshaft engines," *Energy*, vol. 191, 116477, 2020. https://doi.org/10.1016/j.energy.2019.116477.

[2] C. Zhang, V. Gümmer, "The potential of helicopter turboshaft engines incorporating highly effective recuperators under various flight conditions," *Aerospace Science and Technology*, vol. 88, pp. 84–94, 2019. https://doi.org/10.1016/j.ast.2019.03.008.

[3] S. Kim, K. Kim, C. Son, "A new transient performance adaptation method for an aero gas turbine engine," *Energy*, vol. 193, 116752, 2020. https://doi.org/10.1016/j.energy.2019.116752.

[4] T. Castiglione, D. Perrone, L. Strafella, A. Ficarella, S. Bova, "Linear Model of a Turboshaft Aero-Engine Including Components Degradation for Control-Oriented Applications," *Energies*, vol. 16, no. 6, 2634, 2023. https://doi.org/10.3390/en16062634.

[5] X. Chen, J. Hong, Y. Wang, Y. Ma, "Fatigue failure analysis of the central-driven bevel gear in a turboshaft engine arising from multi-source excitation," *Engineering Failure Analysis*, vol. 119, 104811, 2021. https://doi.org/10.1016/j.engfailanal.2020.104811.

[6] Y. Sha, J. Zhao, X. Luan, X. Liu, "Fault feature signal extraction method for rolling bearings in gas turbine engines based on threshold parameter decision screening," *Measurement*, vol. 231, 114567, 2024. https://doi.org/10.1016/j.measurement.2024.114567.

[7] B. Wang, F. Wang, X. Zhang, J. Wang, T. Xue, "Numerical analysis of cooling efficiency for turboshaft engines with converging-diverging film cooling holes," *International Journal of Thermal Sciences*, vol. 185, 108044, 2023. https://doi.org/10.1016/j.ijthermalsci.2022.108044.

[8] Y. Wang, Q. Zheng, Z. Du, H. Zhang, "Research on nonlinear model predictive control for turboshaft engines based on double engines torques matching," *C hinese Journal of Aeronautics*, vol. 33, no. 2, pp. 561–571, 2020. https://doi.org/10.1016/j.cja.2019.10.008.

[9] A. de Voogt, E. St. Amour, "Safety of twin-engine helicopters: Risks and operational specificity," *Safety Science*, vol. 136, 105169, 2021. https://doi.org/10.1016/j.ssci.2021.105169.

[10] L. Sheng-nan, W. Jing-lin, Y. Le, ZhangShang-tian, "Classification of helicopter's typical flight state based on threshold," *IOP Conference Series: Materials Science and Engineering*, vol. 1207, no. 1, 012024, 2021. https://doi.org/10.1088/1757-899X/1207/1/012024.

[11] I. Arush, M. D. Pavel, M. Mulder, "A singular values approach in helicopter gas turbine engines flight testing analysis," *Proceedings of the Institution of Mechanical Engineers, Part G: Journal of Aerospace Engineering*, vol. 234, no. 12, pp. 1851–1865, 2020. https://doi.org/10.1177/0954410020920060.

[12] Z. Yu, X. Yan, R. Chen, "Prediction of pilot workload in helicopter landing after one engine failure," *Chinese Journal of Aeronautics*, vol. 33, no. 12, pp. 3112–3124, 2020. https://doi.org/10.1016/j.cja.2020.05.021

[13] Q. Zheng, Z. Xu, H. Zhang, Z. Zhu, "A turboshaft engine NMPC scheme for helicopter autorotation recovery maneuver," *Aerospace Science and Technology*, vol. 76, pp. 421–432, 2018. https://doi.org/10.1016/j.ast.2018.01.034.

[14] W. El Khatiri, R. Cherif, K. El Bikri, N. Atalla, "Experimental study of component-based transfer path analysis hybrid methods applied to a helicopter," *Applied Acoustics*, vol. 210, 109431, 2023. https://doi.org/10.1016/j.apacoust.2023.109431.

[15] V. Vasiliev, S. Zhernakov, "Classification of gas turbine engine operating modes using neural network technology," Bulletin of USATU, vol. 12, no. 1 (30), pp. 61–74, 2009.

[16] S. Kim, J. H. Im, M. Kim, J. Kim, Y. I. Kim, "Diagnostics using a physics-based engine model in aero gas turbine engine verification tests," *Aerospace Science and Technology*, vol. 133, 108102, 2023. https://doi.org/10.1016/j.ast.2022.108102.

[17] R. Singh, A. Maity, B. Somani, P. S. V. Nataraj, "On-board Fault Diagnosis of a Laboratory Mini SR-30 Gas Turbine Engine," *IFAC-PapersOnLine*, vol. 55, no. 22pp. 153–158, 2022. https://doi.org/10.1016/j.ifacol.2023.03.026.

[18] H. Zhao, Z. Liao, J. Liu, M. Li, W. Liu, L. Wang, Z. Song, "A highly robust thrust estimation method with dissimilar redundancy framework for gas turbine engine," *Energy*, vol. 245, 123255, 2022. https://doi.org/10.1016/j.energy.2022.123255 .

[19] Z. Gu, Q. Li, S. Pang, W. Zhou, J. Wu, C. Zhang, "Turbo-shaft engine adaptive neural network control based on nonlinear state space equation," *Chinese Journal of Aeronautics*, vol. 37, no. 4, pp. 493–507, 2024. https://doi.org/10.1016/j.cja.2023.08.012.

[20] B. Li, Y.-P. Zhao, "Group reduced kernel extreme learning machine for fault diagnosis of aircraft engine," *Engineering Applications of Artificial Intelligence*, vol. 96, 103968, 2020. https://doi.org/10.1016/j.engappai.2020.103968.

[21] S. S. Talebi, A. Madadi, A. M. Tousi, M. Kiaee, "Micro Gas Turbine fault detection and isolation with a combination of Artificial Neural Network and off-design performance analysis," *Engineering Applications of Artificial Intelligence*, vol. 113, 104900, 2022. https://doi.org/10.1016/j.engappai.2022.104900.

[22] S. Sina Tayarani-Bathaie, K. Khorasani, "Fault detection and isolation of gas turbine engines using a bank of neural networks," *Journal of Process Control*, vol. 36, pp. 22–41, 2015. https://doi.org/10.1016/j.jprocont.2015.08.007.

[23] S. Togni, T. Nikolaidis, S. Sampath, "A combined technique of Kalman filter, artificial neural network and fuzzy logic for gas turbines and signal fault isolation," *Chinese Journal of Aeronautics*, vol. 34, no. 2, pp. 124–135, 2021. https://doi.org/10.1016/j.cja.2020.04.015.

[24] Y. Shen, K. Khorasani, "Hybrid multi-mode machine learning-based fault diagnosis strategies with application to aircraft gas turbine engines," *Neural Networks*, vol. 130, pp. 126–142, 2020. https://doi.org/10.1016/j.neunet.2020.07.001.

[25] S. Pang, Q. Li, B. Ni, "Improved nonlinear MPC for aircraft gas turbine engine based on semi-alternative optimization strategy," *Aerospace Science and Technology*, vol. 118, 106983, 2021. https://doi.org/10.1016/j.ast.2021.106983.

[26] B. Li, Y.-P. Zhao, Y.-B. Chen, "Unilateral alignment transfer neural network for fault diagnosis of aircraft engine," *Aerospace Science and Technology*, vol. 118, 107031, 2021. https://doi.org/10.1016/j.ast.2021.107031.

[27] Z. Xu, J. H. Saleh, R. Subagia, "Machine learning for helicopter accident analysis using supervised classification: Inference, prediction, and implications," *Reliability Engineering & System Safety*, vol. 204, 107210, 2020. https://doi.org/10.1016/j.ress.2020.107210.

[28] Y. Jiang, L. Liu, G. Feng, "Fully distributed adaptive control for output consensus of uncertain discrete-time linear multi-agent systems," *Automatica*, vol. 162, 111531, 2024. https://doi.org/10.1016/j.automatica.2024.111531.

[29] S. Vladov, L. Scislo, V. Sokurenko, O. Muzychuk, V. Vysotska, A. Sachenko, A. Yurko, "Helicopter Turboshaft Engines' Gas Generator Rotor R.P.M. Neuro-Fuzzy On-Board Controller Development," *Energies*, vol. 17, issue 16, 4033, 2024. https://doi.org/10.3390/en17164033.

[30] S. Vladov, Y. Shmelov, R. Yakovliev, "Modified Neural Network Method for Classifying the Helicopters Turboshaft Engines Ratings at Flight Modes," *Proceedings of the 2022 IEEE 41st International Conference on Electronics and Nanotechnology (ELNANO)*, Kyiv, Ukraine, October 10–14, 2022, pp. 535–540. https://doi.org/10.1109/ELNANO54667.2022.9927108.

[31] X. Liu, Y.Chen, L. Xiong, J. Wang, C. Luo, L. Zhang, K. Wang, "Intelligent fault diagnosis methods toward gas turbine: A review," Chinese Journal of Aeronautics, vol. 37, no. 4, pp. 93–120, 2024. https://doi.org/10.1016/j.cja.2023.09.024.

[32] J. Xie, M. Sage, Y. F. Zhao, "Feature selection and feature learning in machine learning applications for gas turbines: A review," *Engineering Applications of Artificial Intelligence*, vol. 117, 105591, 2023. https://doi.org/10.1016/j.engappai.2022.105591.

[33] M. Razmjooei, F. Ommi, Z. Saboohi, "Experimental analysis and modeling of gas turbine engine performance: Design point and off-design insights through system of equations solutions," *Results in Engineering*, vol. 23, 102495, 2024. https://doi.org/10.1016/j.rineng.2024.102495.

[34] K. Andriushchenko, V. Rudyk, O. Riabchenko, M. Kachynska, N. Marynenko, L. Shergina, V. Kovtun, M. Tepliuk, A. Zhemba, O. Kuchai, "Processes of managing information infrastructure of a digital enterprise in the framework of the «Industry 4.0» concept," *Eastern-European Journal of Enterprise Technologies*, vol. 1, no. 3 (97), pp. 60–72, 2019. https://doi.org/10.15587/1729-4061.2019.157765.

[35] E. Tsoutsanis, N. Meskin, "Performance assessment of classical and fractional controllers for transient operation of gas turbine engines," *IFAC-PapersOnLine*, vol. 51, no. 4, pp. 687–692, 2018. https://doi.org/10.1016/j.ifacol.2018.06.182.

[36] S. Vladov, L. Scislo, V. Sokurenko, O. Muzychuk, V. Vysotska, S. Osadchy, A. Sachenko, "Neural Network Signal Integration from Thermogas-Dynamic Parameter Sensors for Helicopters Turboshaft Engines at Flight Operation Conditions," *Sensors*, vol. 24, no. 13, 4246, 2024. https://doi.org/10.3390/s24134246.

[37] I. M. A. Ibrahem, O. Akhrif, H. Moustapha, M. Staniszewski, "Nonlinear generalized predictive controller based on ensemble of NARX models for industrial gas turbine engine," *Energy*, vol. 230, 120700, 2021. https://doi.org/10.1016/j.energy.2021.120700.

[38] S. Babichev, J. Krejci, J. Bicanek, V. Lytvynenko, "Gene expression sequences clustering based on the internal and external clustering quality criteria," *Proceedings of the 2017 12th International Scientific and Technical Conference on Computer Sciences and Information Technologies (CSIT)*, Lviv, Ukraine, 05–08 September 2017. https://doi.org/10.1109/STC-CSIT.2017.8098744.

[39] Z. Hu, E. Kashyap, O. K. Tyshchenko, "GEOCLUS: A Fuzzy-Based Learning Algorithm for Clustering Expression Datasets," *Lecture Notes on Data Engineering and Communications Technologies*, pp. 337–349, 2022. https://doi.org/10.1007/978-3-031-04812-8_29.

[40] S. Vladov, R. Yakovliev, M. Bulakh, V. Vysotska, "Neural Network Approximation of Helicopter Turboshaft Engine Parameters for Improved Efficiency," *Energies*, vol. 17, no. 9, 2233, 2024. https://doi.org/10.3390/en17092233.

[41] S. Vladov, R. Yakovliev, V. Vysotska, M. Nazarkevych, V. Lytvyn, "The Method of Restoring Lost Information from Sensors Based on Auto-Associative Neural Networks," *Applied System Innovation*, vol. 7, no. 3, 53, 2024. https://doi.org/10.3390/asi7030053.

[42] L. Song, Y. Liu, J. Fan, D.-X. Zhou, "Approximation of smooth functionals using deep ReLU networks," *Neural Networks*, vol. 166, pp. 424–436, 2023. https://doi.org/10.1016/j.neunet.2023.07.012.

[43] S. Vladov, Y. Shmelov, R. Yakovliev, "Methodology for Control of Helicopters Aircraft Engines Technical State in Flight Modes Using Neural Networks," *CEUR Workshop Proceedings*, vol. 3137, pp. 108–125, 2022. https://doi.org/10.32782/cmis/3137-10.

[44] P. V. de Campos Souza, M. Dragoni, "IFNN: Enhanced interpretability and optimization in FNN via Adam algorithm," *Information Sciences*, vol. 678, 121002, 2024. https://doi.org/10.1016/j.ins.2024.121002.

[45] R. M. Catana, G. Dediu, "Analytical Calculation Model of the TV3-117 Turboshaft Working Regimes Based on Experimental Data," *Applied Sciences*, vol. 13, no. 19, 10720, 2023. https://doi.org/10.3390/app131910720.

[46] R. M. Catană, G. Dediu, and C. M. Tărăbîc, "Studies and Experimental Research in the Evaluation of TV2-117A Turboshaft Engine Working Regimes," *Applied Sciences*, vol. 12, no. 7, 3703, 2022. https://doi.org/10.3390/app12073703.

[47] M. Montazeri-Gh and S. Yazdani, "Application of interval type-2 fuzzy logic systems to gas turbine fault diagnosis," *Applied Soft Computing*, vol. 96, 106703, 2020. https://doi.org/10.1016/j.asoc.2020.106703.

[48] L. Gebrehiwet, Y. Nigussei, T. Teklehaynanot, "A Review-Differentiating TV2 and TV3 Series Turbo Shaft Engines," *International Journal of Research Publication and Reviews. Genesis Global Publication*, vol. 3, no. 8, pp. 1822–1839, 2022. https://doi.org/10.55248/gengpi.2022.3.8.55.

[49] Z.-Q. Li, Y.-P. Zhao, Z.-Y. Cai, P.-P. Xi, Y.-T. Pan, G. Huang, T.-H. Zhang, "A proposed self-organizing radial basis function network for aero-engine thrust estimation," *Aerospace Science and Technology*, vol. 87, pp. 167–177, 2019. https://doi.org/10.1016/j.ast.2019.01.033.

[50] S. D. Bolboacă, L. Jäntschi, A. F. Sestraș, R. E. Sestraș, D. C. Pamfil, "Pearson-Fisher Chi-Square Statistic Revisited," *Information*, vol. 2, no. 3, pp. 528–545, 2011. https://doi.org/10.3390/info2030528.

[51] F. Avram, N. N. Leonenko, N. Šuvak, "Hypothesis testing for Fisher–Snedecor diffusion," *Journal of Statistical Planning and Inference*, vol. 142, no. 8, pp. 2308–2321, 2012. https://doi.org/10.1016/j.jspi.2012.02.055.

[52] S. Zhang, A. Ma, T. Zhang, N. Ge, X. Huang, "A Performance Simulation Methodology for a Whole Turboshaft Engine Based on Throughflow Modelling," *Energies*, vol. 17, no. 2, 494, 2024. https://doi.org/10.3390/en17020494.

[53] J. Tang, H. Li, J. Zhang, K. Guan, Q. Shan, X. Liang, "A robust PID and RLS controller for TCP/AQM system," *Journal of Network and Computer Applications*, vol. 229, 103947, 2024. https://doi.org/10.1016/j.jnca.2024.103947.

[54] H. Feng, B. Liu, M. Xu, M. Li, Z. Song, "Model-based deduction learning control: A novel method for optimizing gas turbine engine afterburner transient," *Energy*, vol. 292, 130512, Apr. 2024. https://doi.org/10.1016/j.energy.2024.130512.

[55] D. Xu, S. Zhang, H. Zhang, D. P. Mandic, "Convergence of the RMSProp deep learning method with penalty for nonconvex optimization," *Neural Networks*, vol. 139, pp. 17–23, 2021. https://doi.org/10.1016/j.neunet.2021.02.011.

[56] M. Pasieka, N. Grzesik, K. Kuźma, "Simulation modeling of fuzzy logic controller for aircraft engines," *International Journal of Computing*, vol. 16, issue 1, pp. 27–33, 2017. https://doi.org/10.47839/ijc.16.1.868.

[57] S. Vladov, R. Yakovliev, O. Hubachov, J. Rud, Y. Stushchanskyi, "Neural Network Modeling of Helicopters Turboshaft Engines at Flight Modes Using an Approach Based on "Black Box" Models," CEUR Workshop Proceedings, vol. 3624, pp. 116–135, 2024. URL: https://ceur-ws.org/Vol-3624/Paper_11.pdf

[58] M. Xu, J. Wang, J. Liu, M. Li, J. Geng, Y. Wu, Z. Song, "An improved hybrid modeling method based on extreme learning machine for gas turbine engine," Aerospace Science and Technology, vol. 107, 106333, 2020. https://doi.org/10.1016/j.ast.2020.106333.

[59] W. Molla Salilew, Z. Ambri Abdul Karim, T. Alemu Lemma, "Investigation of fault detection and isolation accuracy of different Machine learning techniques with different data processing methods for gas turbine," Alexandria Engineering Journal, vol. 61, no. 12, pp. 12635–12651, 2022. https://doi.org/10.1016/j.aej.2022.06.026.

[60] H. Sheng, Q. Chen, J. Li, W. Jiang, Z. Wang, Z. Liu, T. Zhang, Y. Liu, "Research on dynamic modeling and performance analysis of helicopter turboshaft engine's start-up process," *Aerospace Science and Technology*, vol. 106, 106097, 2020. https://doi.org/10.1016/j.ast.2020.106097.

[61] S. Vladov, Y. Shmelov, R. Yakovliev, M. Petchenko, "Neural Network Method for Parametric Adaptation Helicopters Turboshaft Engines On-Board Automatic Control System Parameters," *CEUR Workshop Proceedings*, vol. 3403, pp. 179–195, 2023. URL: https://ceur-ws.org/Vol-3403/paper15.pdf

[62] A. R. Marakhimov, K. K. Khudaybergenov, "Approach to the synthesis of neural network structure during classification," *International Journal of Computing*, vol. 19, issue 1, pp. 20–26, 2020. https://doi.org/10.47839/ijc.19.1.1689.

[63] Y. Wang, Z. Wang, "Model free adaptive fault-tolerant tracking control for a class of discrete-time systems," Neurocomputing, vol. 412., pp. 143–151, 2020. https://doi.org/10.1016/j.neucom.2020.06.027.

[64] E. M. Cherrat, R. Alaoui, H. Bouzahir, "Score fusion of finger vein and face for human recognition based on convolutional neural network model," *International Journal of Computing*, vol. 19, issue 1, pp. 11–19, 2020. https://doi.org/10.47839/ijc.19.1.1688.

[65] E. L. Ntantis, P. N. Botsaris, "Diagnostic Methods for an Aircraft Engine Performance," *Journal of Engineering Science and Technology Review*, vol. 8, no. 4, pp. 64–72, 2015. https://doi.org/10.25103/jestr.084.10.

[66] Y. Shmelov, S. Vladov, Y. Klimova, M. Kirukhina, "Expert system for identification of the technical state of the aircraft engine TV3-117 in flight modes," *Proceedings of the 2017 System Analysis & Intelligent Computing: IEEE First International Conference on System Analysis & Intelligent Computing (SAIC)*, Kyiv, Ukraine, 08–12 October 2018, pp. 77–82. https://doi.org/10.1109/SAIC.2018.8516864.

[67] Y. Wei, R. Chen, Y. Yuan, L. Wang, "Influence of Engine Dynamic Characteristics on Helicopter Handling Quality in Hover and Low-Speed Forward Flight," *Aerospace*, vol. 11, no. 1, 34, 2023. https://doi.org/10.3390/aerospace11010034.

[68] A. de Voogt, K. Nero, "Technical Failures in Helicopters: Non-Powerplant-Related Accidents," *Safety*, vol. 9, no. 1, 40, 2023. https://doi.org/10.3390/safety9010010.

[69] I. G. Castillo, I. Loboda, and J. L. Pérez Ruiz, "Data-Driven Models for Gas Turbine Online Diagnosis," *Machines*, vol. 9, no. 12, 372, 2021. https://doi.org/10.3390/machines9120372.

[70] V. Venkatesh, K. Raghavendra, M. Madan, M. Sujata, S. K. Bhaumik, "Failure analysis of non-rotating control rod of a helicopter," *Procedia Structural Integrity*, vol. 60, pp. 372–381, 2024. https://doi.org/10.1016/j.prostr.2024.05.058.

[71] A. Sachenko, V. Kochan, R. Kochan, V. Turchenko, K. Tsahouridis, and T. Laopoulos, "Error compensation in an intelligent sensing instrumentation system," *IMTC 2001. Proceedings of the 18th IEEE Instrumentation and Measurement Technology Conference. Rediscovering Measurement in the Age of Informatics*, Budapest, Hungary, May, 21–23, 2001, vol. 2, pp. 869–874. https://doi.org/10.1109/IMTC.2001.928201.

[72] N. Vasylkiv, L. Dubchak, and A. Sachenko, "Estimation method of information system functioning quality based on the fuzzy logic," *CEUR Workshop Proceedings*, vol. 2631, pp. 40–56, 2020. https://ceur-ws.org/Vol-2631/paper4.pdf.

[73] D. Vlasenko, O. Inkarbaieva, M. Peretiatko, D. Kovalchuk, O. Sereda, "Helicopter radio system for low altitudes and flight speed measuring with pulsed ultra-wideband stochastic sounding signals and artificial intelligence elements," Radioelectronic and Computer Systems, no. 3, pp. 48–59, 2023. https://doi.org/10.32620/reks.2023.3.05.

***SERHII VLADOV** is a Head of the Department of Scientific Work Organization and Gender Issues at Kremenchuk Flight College of Kharkiv National University of Internal Affairs. He is Candidate in Technical Sciences. His current research and the fields of specialization – development of applied intelligent systems (including intelligent automatic control systems) of complex dynamic objects, in particular, helicopter turboshaft engines. He has nearly 200 scientific papers, among them more than 30, which are indexed in the Scopus scientific database.*

***ZHADYRA AVKUROVA** is the Lecturer of Department of AI Technology at NAO Karaganda Industrial University and PhD student at L.N. Gumilyov Eurasian National University, Kazakhstan. Major research interests: information technology, information security, cybersecurity, APT-attacks detection, fuzzy logic, AI/ML-based security systems.*

***VASYL LYTVYN** is the Head of the Information Systems and Networks Department in Lviv Polytechnic National University, Full Professor, Doctor of Technical Sciences. He has a total work experience of 22 years, with research and educational experience. Lytvyn V. is an expert in Data Science, Big Data, ontological engineering; participated in many researches as a performer and supervisor. He has more than 300 scientific publications.*

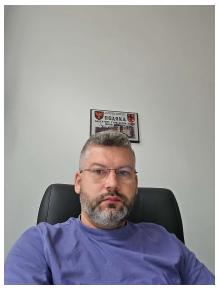

***Yurii Zhovnir** aspirant at Information systems and network department of the National university Lviv Polytechnic. CEO at ISP Astra (Lviv, Ukraine). The scientfic interests includes computer network and security system, artificial intelligent systems. Other interests are: business, finance.*